RECENT ADVANCES ON THE DESIGN OF UPWIND FLUXES

Eleuterio TORO
Laboratory of Applied Mathematics
University of Trento, Italy
www.ing.unitn.it/toro
toro@ing.unitn.it

August 26, 2012

Aim of this lecture:

to present some very recent developments on upwind fluxes for hyperbolic equations

- Part A: Generalization of the Osher-Solomon Riemann solver (with Michael Dumbser)
- Part B: New flux vector splitting type schemes (with Maria E. Vázquez-Cendón)

REFERENCES:

Michael Dumbser and Eleuterio Toro.
A simple extension of the Osher Riemann solver to general non-conservative hyperbolic systems.
Journal of Scientific Computing, Vol. 48, Issue 1-3, pp 70-88, 2011.

Michael Dumbser and Eleuterio Toro.
On universal Osher-type schemes for general nonlinear hyperbolic conservation laws.
Communications in Computational Physics. Vol. 10, pp 635-671, 2011.

E F Toro and M Dumbser.
Reformulated Osher-type Riemann solver.
Computational Fluid Dynamics 2010. Springer-Verlag, Alexan- der Kuzmin (editor), 2011, pp 131-136.

Bok Jik Lee, Eleuterio F. Toro,
Cristobal E. Castro and Nikos Nikiforakis.
Adaptive Osher-type scheme for the Euler equations with highly nonlinear equations of state.
Journal of Computational Physics. Submitted, August 2012.

E F Toro and M E Vázquez-Cendón.
Flux splitting schemes for the Euler equations.
Computers and Fluids. (Accepted, 2012).

Part A:
A generalization of the Osher-Solomon Riemann solver

DOT: Dumbser-Osher-Toro solver

Method is applicable to any hyperbolic system.

There are 2 cases:

- Eigenstructure, analytically available. Use it.

- Eigenstructure, NOT analytically available. Compute it numerically and use it.

A1. INTRODUCTION

$$\partial_t \mathbf{Q} + \partial_x \mathbf{F}(\mathbf{Q}) = \mathbf{0} \tag{1}$$

$$\mathbf{Q} = [q_1, q_2, ..., q_m]^T, \quad \mathbf{F}(\mathbf{Q}) = [f_1, f_2, ..., f_m]^T$$

$$\text{Jacobian matrix: } \mathbf{A}(\mathbf{Q}) = \frac{\partial \mathbf{F}(\mathbf{Q})}{\partial \mathbf{Q}}$$

$$\text{Eigenvalues: } \lambda_1(\mathbf{Q}), \lambda_2(\mathbf{Q}), \ldots, \lambda_m(\mathbf{Q})$$

$$\text{Right eigenvectors: } \mathbf{R}_1(\mathbf{Q}), \mathbf{R}_2(\mathbf{Q}), \ldots, \mathbf{R}_m(\mathbf{Q})$$

Jacobian matrix is diagonalizable:

$$\mathbf{A}(\mathbf{Q}) = \mathbf{R}(\mathbf{Q})\mathbf{\Lambda}(\mathbf{Q})\mathbf{R}(\mathbf{Q})^{-1} \tag{2}$$

$\mathbf{R}(\mathbf{Q})$: matrix of right eigenvectors

$\mathbf{R}(\mathbf{Q})^{-1}$: inverse of $\mathbf{R}(\mathbf{Q})$

$\mathbf{\Lambda}(\mathbf{Q})$: diagonal matrix, diagonal entries are the eigenvalues.

Conservative scheme:

$$\mathbf{Q}_i^{n+1} = \mathbf{Q}_i^n - \frac{\Delta t}{\Delta x}\left(\mathbf{F}_{i+\frac{1}{2}} - \mathbf{F}_{i-\frac{1}{2}}\right) \tag{3}$$

Numerical flux: $\mathbf{F}_{i+\frac{1}{2}}$ computed by solving:

The Riemann problem

$$\left.\begin{array}{l} \partial_t \mathbf{Q} + \partial_x \mathbf{F}(\mathbf{Q}) = \mathbf{0} \\ \\ \mathbf{Q}(x,0) = \left\{ \begin{array}{lll} \mathbf{Q}_0 \equiv \mathbf{Q}_i^n, & if & x < 0, \\ \\ \mathbf{Q}_1 \equiv \mathbf{Q}_{i+1}^n, & if & x > 0. \end{array} \right. \end{array}\right\} \tag{4}$$

Riemann solvers:

- Exact Riemann solver (Godunov 1959)
- Linearised Riemann solver of Godunov (1960)
- One-wave solver of Rusanov (1961)
- Linearised Riemann solver of Roe (1981)
- Non-linear solver of Osher-Solomon (1982)
- Two-wave solver of Harten-Lax-van Leer (1983)
- Variations of HLL: HLLE, HLLEM
- HLLC (many-wave solver)
- Other approaches (eg FVS)

Centred fluxes (0-wave models):

- Flux of Lax-Friedrichs (1960)
- FORCE flux of Toro (1996) (related to scheme of Tadmor and collaborators)

Toro E F. Riemann solvers and numerical methods for fluid dynamics. Springer, Third Edition, 2009.

We now introduce the definitions

$$\lambda_i^+(\mathbf{Q}) = \max(\lambda_i(\mathbf{Q}), 0)\ , \quad \lambda_i^-(\mathbf{Q}) = \min(\lambda_i(\mathbf{Q}), 0) \tag{5}$$

Note that

$$\left.\begin{aligned} |\lambda_i(\mathbf{Q})| &= \lambda_i^+(\mathbf{Q}) - \lambda_i^-(\mathbf{Q})\ , \\ \lambda_i(\mathbf{Q}) &= \lambda_i^+(\mathbf{Q}) + \lambda_i^-(\mathbf{Q})\ . \end{aligned}\right\} \tag{6}$$

and hence

$$\left.\begin{aligned} |\mathbf{\Lambda}(\mathbf{Q})| &= \mathbf{\Lambda}^+(\mathbf{Q}) - \mathbf{\Lambda}^-(\mathbf{Q})\ , \\ \mathbf{\Lambda}(\mathbf{Q}) &= \mathbf{\Lambda}^+(\mathbf{Q}) + \mathbf{\Lambda}^-(\mathbf{Q})\ . \end{aligned}\right\} \tag{7}$$

Then the diagonalization process is extended as

$$\left.\begin{aligned} \mathbf{A}^{+}(\mathbf{Q}) &= \mathbf{R}(\mathbf{Q})\mathbf{\Lambda}^{+}(\mathbf{Q})\mathbf{R}^{-1}(\mathbf{Q})\,, \\ \mathbf{A}^{-}(\mathbf{Q}) &= \mathbf{R}(\mathbf{Q})\mathbf{\Lambda}^{-}(\mathbf{Q})\mathbf{R}^{-1}(\mathbf{Q})\,, \\ |\mathbf{A}(\mathbf{Q})| &= \mathbf{R}(\mathbf{Q})|\mathbf{\Lambda}(\mathbf{Q})|\mathbf{R}^{-1}(\mathbf{Q})\,. \end{aligned}\right\} \tag{8}$$

It follows that

$$\left.\begin{aligned} |\mathbf{A}(\mathbf{Q})| &= \mathbf{A}^{+}(\mathbf{Q}) - \mathbf{A}^{-}(\mathbf{Q})\,, \\ \mathbf{A}(\mathbf{Q}) &= \mathbf{A}^{+}(\mathbf{Q}) + \mathbf{A}^{-}(\mathbf{Q})\,. \end{aligned}\right\} \tag{9}$$

A2. THE OSHER-SOLOMON FLUX (1982) BRIEF REVIEW

Chapter 12 of
Toro E F. Riemann solvers and numerical methods for fluid dynamics. Springer, Third Edition, 2009.

The Osher-Solomon numerical flux (1982) is obtained by first assuming the flux splitting

$$\mathbf{F}(\mathbf{Q}) = \mathbf{F}^{+}(\mathbf{Q}) + \mathbf{F}^{-}(\mathbf{Q}) \,, \tag{10}$$

with corresponding Jacobians

$$\mathbf{A}^{+}(\mathbf{Q}) = \frac{\partial \mathbf{F}^{+}(\mathbf{Q})}{\partial \mathbf{Q}} \,, \quad \mathbf{A}^{-}(\mathbf{Q}) = \frac{\partial \mathbf{F}^{-}(\mathbf{Q})}{\partial \mathbf{Q}} \,. \tag{11}$$

The Osher-Solomon flux is defined as

$$\mathbf{F}_{i+\frac{1}{2}}(\mathbf{Q}_0, \mathbf{Q}_1) = \mathbf{F}^{+}(\mathbf{Q}_0) + \mathbf{F}^{-}(\mathbf{Q}_1) \,. \tag{12}$$

From (11) we may write the integral relations

$$\int_{\mathbf{Q}_0}^{\mathbf{Q}_1} \mathbf{A}^-(\mathbf{Q}) d\mathbf{Q} = \mathbf{F}^-(\mathbf{Q}_1) - \mathbf{F}^-(\mathbf{Q}_0) \tag{13}$$

and

$$\int_{\mathbf{Q}_0}^{\mathbf{Q}_1} \mathbf{A}^+(\mathbf{Q}) d\mathbf{Q} = \mathbf{F}^+(\mathbf{Q}_1) - \mathbf{F}^+(\mathbf{Q}_0) \, . \tag{14}$$

Then we can express (12) in three different forms, namely

$$\mathbf{F}_{i+\frac{1}{2}} = \mathbf{F}(\mathbf{Q}_0) + \int_{\mathbf{Q}_0}^{\mathbf{Q}_1} \mathbf{A}^{-}(\mathbf{Q}) d\mathbf{Q} \,, \tag{15}$$

$$\mathbf{F}_{i+\frac{1}{2}} = \mathbf{F}(\mathbf{Q}_1) - \int_{\mathbf{Q}_0}^{\mathbf{Q}_1} \mathbf{A}^{+}(\mathbf{Q}) d\mathbf{Q} \tag{16}$$

and

$$\mathbf{F}_{i+\frac{1}{2}} = \frac{1}{2}(\mathbf{F}(\mathbf{Q}_0) + \mathbf{F}(\mathbf{Q}_1)) - \frac{1}{2} \int_{\mathbf{Q}_0}^{\mathbf{Q}_1} |\mathbf{A}(\mathbf{Q})| d\mathbf{Q} \,. \tag{17}$$

To obtain (20), for example, we use (24) to write

$$\mathbf{F}(\mathbf{Q}_0) = \mathbf{F}^+(\mathbf{Q}_0) + \mathbf{F}^-(\mathbf{Q}_0)\ .$$

Then, writing (12) as

$$\left.\begin{aligned}
\mathbf{F}_{i+\frac{1}{2}} &= \mathbf{F}^+(\mathbf{Q}_0) + \mathbf{F}^-(\mathbf{Q}_1) + \mathbf{F}(\mathbf{Q}_0) - \mathbf{F}(\mathbf{Q}_0) \\
&= \mathbf{F}(\mathbf{Q}_0) + \mathbf{F}^+(\mathbf{Q}_0) + \mathbf{F}^-(\mathbf{Q}_1) - \mathbf{F}(\mathbf{Q}_0) \\
&= \mathbf{F}(\mathbf{Q}_0) + \mathbf{F}^+(\mathbf{Q}_0) + \mathbf{F}^-(\mathbf{Q}_1) - (\mathbf{F}^+(\mathbf{Q}_0) + \mathbf{F}^-(\mathbf{Q}_0)) \\
&= \mathbf{F}(\mathbf{Q}_0) + \mathbf{F}^-(\mathbf{Q}_1) - \mathbf{F}^-(\mathbf{Q}_0) \\
&= \mathbf{F}(\mathbf{Q}_0) + \int_{\mathbf{Q}_0}^{\mathbf{Q}_1} \mathbf{A}^-(\mathbf{Q}) d\mathbf{Q}\ .
\end{aligned}\right\} \quad (18)$$

and using (14) expression (20) follows.

Osher's flux from

$$\mathbf{F}_{i+\frac{1}{2}} = \mathbf{F}(\mathbf{Q}_0) + \int_{\mathbf{Q}_0}^{\mathbf{Q}_1} \mathbf{A}^-(\mathbf{Q}) d\mathbf{Q} \ , \tag{19}$$

To evaluate the integral in phase space one requires a *path*
One selects the path so as to make the integration tractable.
A path $\mathbf{I}(\mathbf{Q})$ connecting the state $\mathbf{Q}_0$ to $\mathbf{Q}_1$ is defined as

$$\mathbf{I}(\mathbf{Q}) = \cup_1^m \mathbf{I}_k(\mathbf{Q}) \ , \tag{20}$$

$\mathbf{Q}_{(k-1)/m}$: intersection points in phase space.

$\mathbf{I}_k(\mathbf{Q})$: *partial* path associated with the k-th field.

Complete details in Chapter 12 of
Toro E F. Riemann solvers and numerical methods for fluid dynamics. Springer, Third Edition, 2009.

A4. GENERALIZATION OF THE OSHER SCHEME

The Osher-Solomon numerical flux (1982) may be defined as

$$\mathbf{F}_{i+\frac{1}{2}} = \frac{1}{2}(\mathbf{F}(\mathbf{Q}_0) + \mathbf{F}(\mathbf{Q}_1)) - \frac{1}{2}\int_{\mathbf{Q}_0}^{\mathbf{Q}_1} |\mathbf{A}(\mathbf{Q})| d\mathbf{Q} \,. \qquad (21)$$

- Evaluation of an integral in phase space is required
- Integration path chosen joining $\mathbf{Q}_0$ to $\mathbf{Q}_1$ required
- Here we first propose to select the canonical path

$$\psi(s; \mathbf{Q}_0, \mathbf{Q}_1) = \mathbf{Q}_0 + s(\mathbf{Q}_1 - \mathbf{Q}_0) \,, \quad s \in [0, 1] \qquad (22)$$

to evaluate the integral in (21).

Note that under a change of variables we obtain

$$\mathbf{F}_{i+\frac{1}{2}} = \frac{1}{2}(\mathbf{F}(\mathbf{Q}_0) + \mathbf{F}(\mathbf{Q}_1)) - \frac{1}{2}\left(\int_0^1 |\mathbf{A}(\psi(s;\mathbf{Q}_0,\mathbf{Q}_1))|\, ds\right)(Q_1 - Q_0)\ . \tag{23}$$

Then we evaluate the integral in (23) *numerically* along path ψ using a Gauss-Legendre quadrature rule with G points s_j and associated weights ω_j in the unit interval $I = [0,1]$,

$$\mathbf{F}_{i+\frac{1}{2}} = \frac{1}{2}(\mathbf{F}(\mathbf{Q}_0) + \mathbf{F}(\mathbf{Q}_1)) - \frac{1}{2}\left(\sum_{j=1}^{G} \omega_j\, |\mathbf{A}(\psi(s_j;\mathbf{Q}_0,\mathbf{Q}_1))|\right)(Q_1 - Q_0)\,. \tag{24}$$

Note that $|\mathbf{A}(\psi(s_j;\mathbf{Q}_0,\mathbf{Q}_1))|$ must be decomposed as in (9) for each s_j

A5. NUMERICAL RESULTS

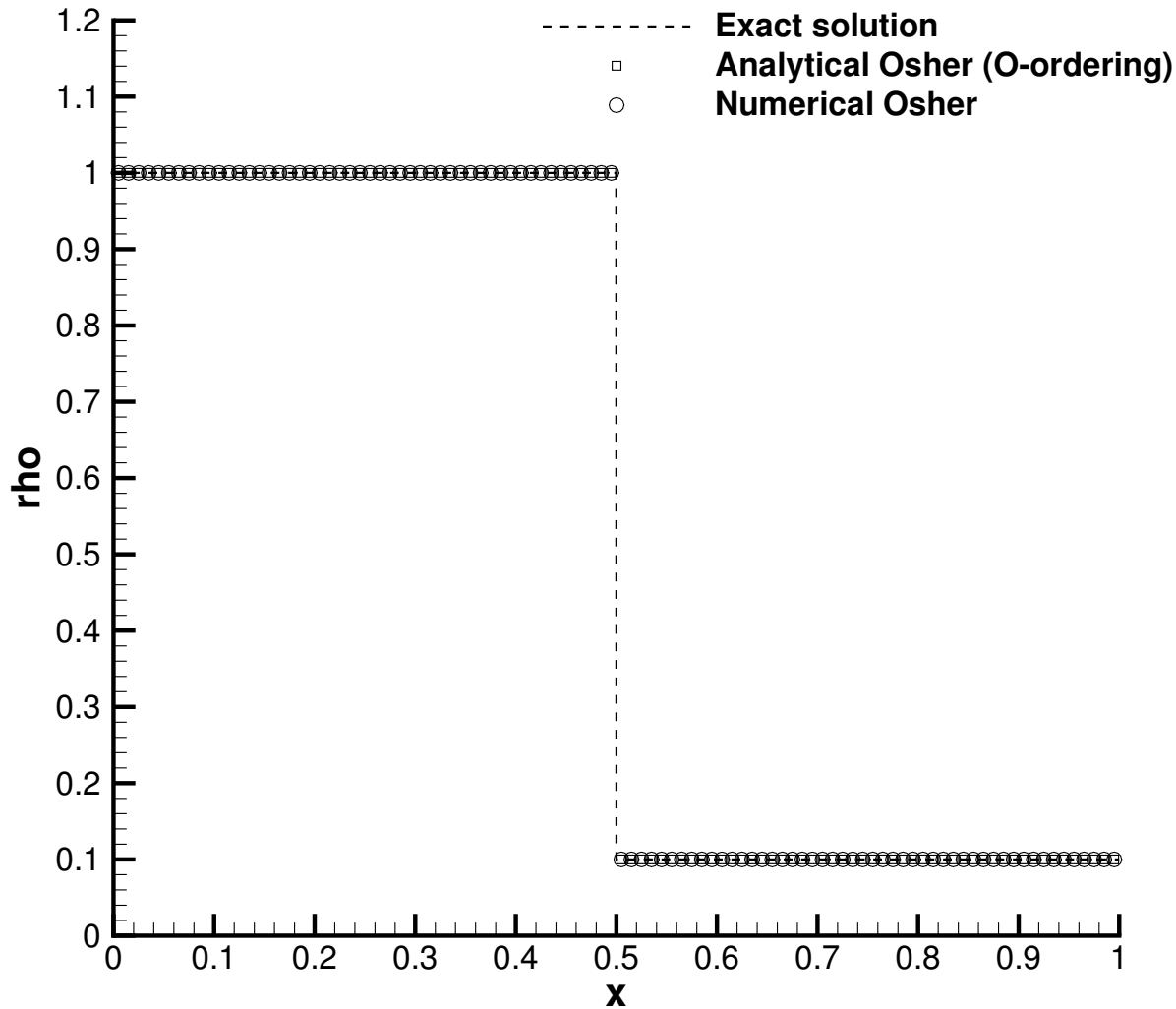

Euler equations: isolated stationary contact.

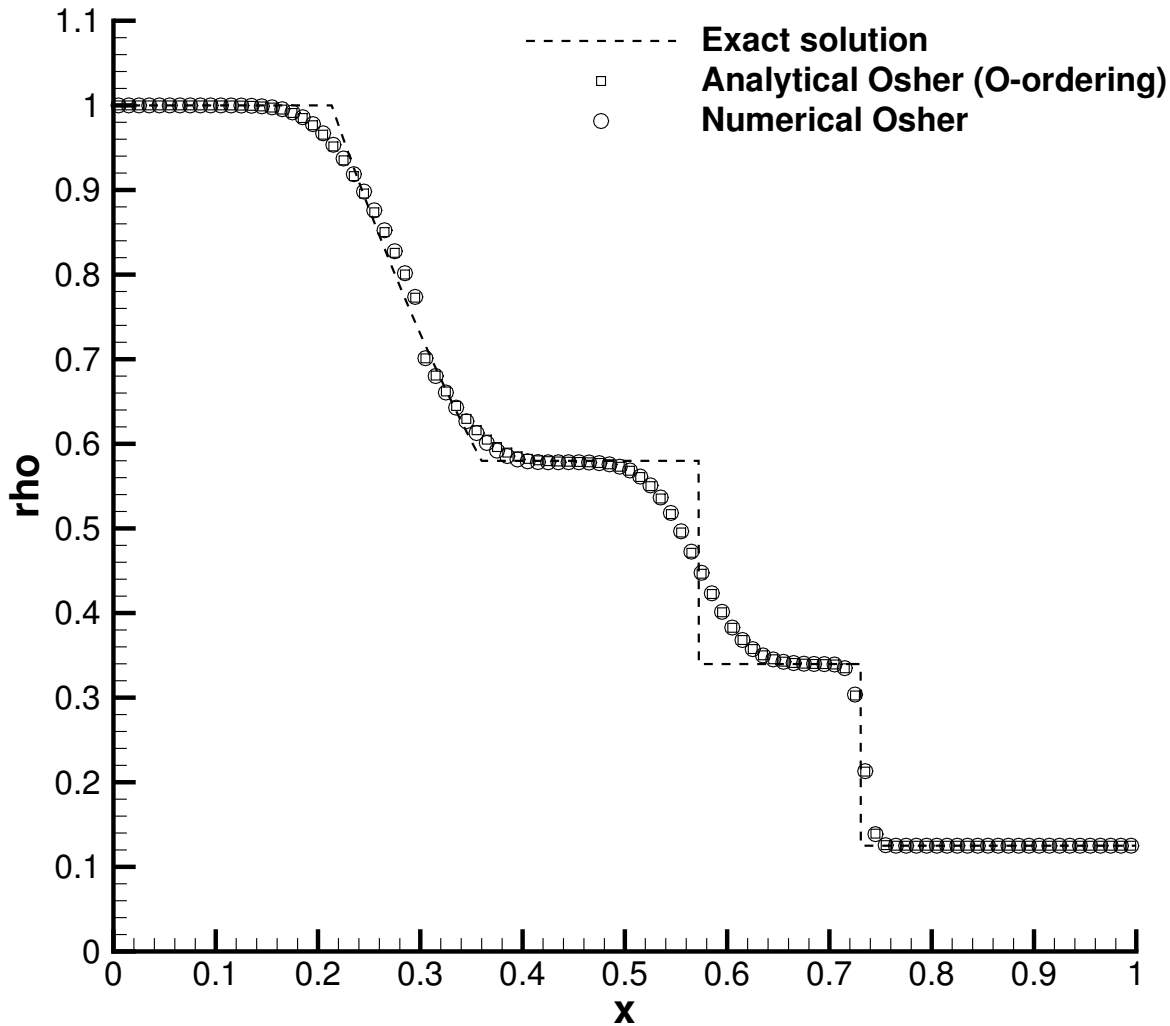

Euler equations: sonic left rarefaction.

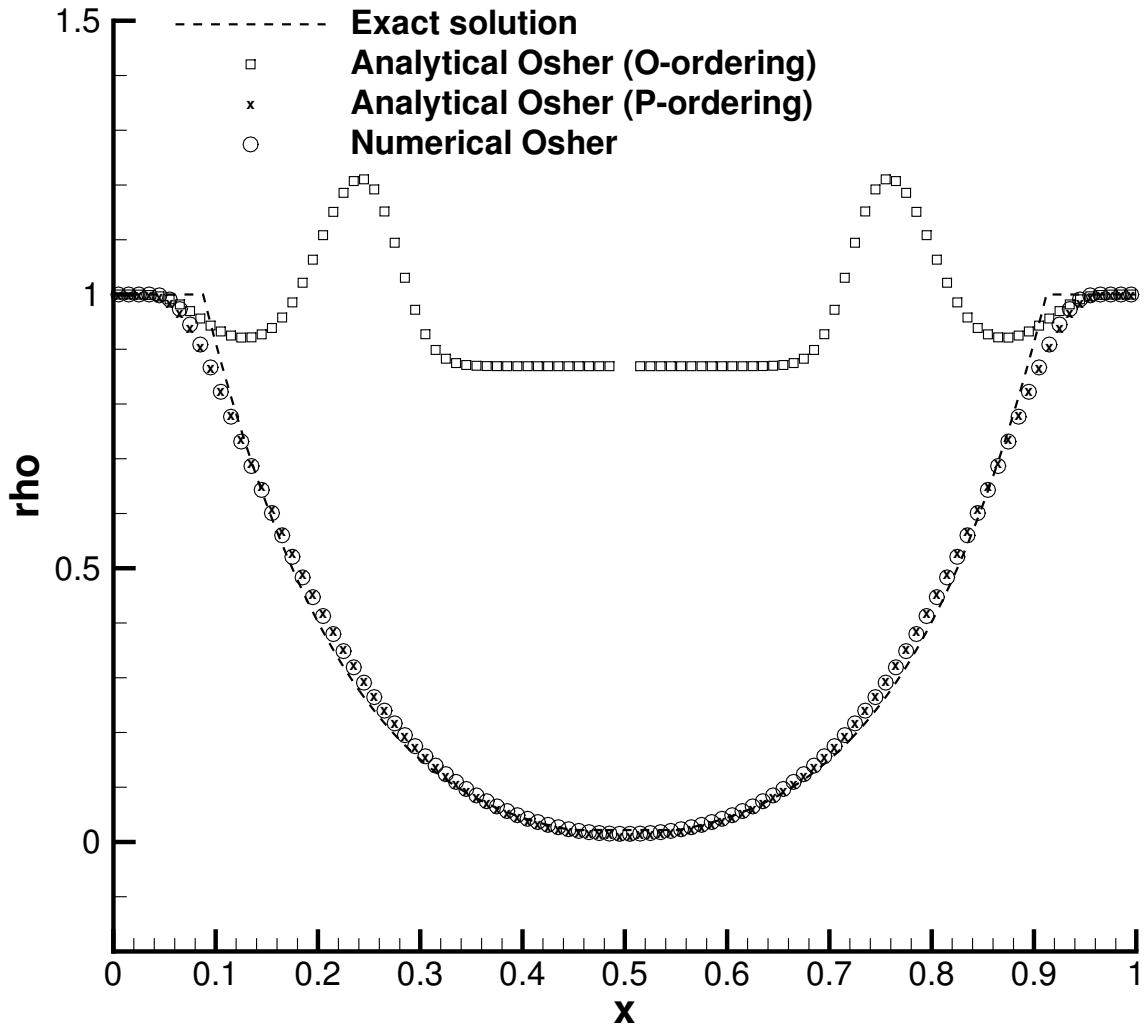

Euler equations: 123 test, low density.

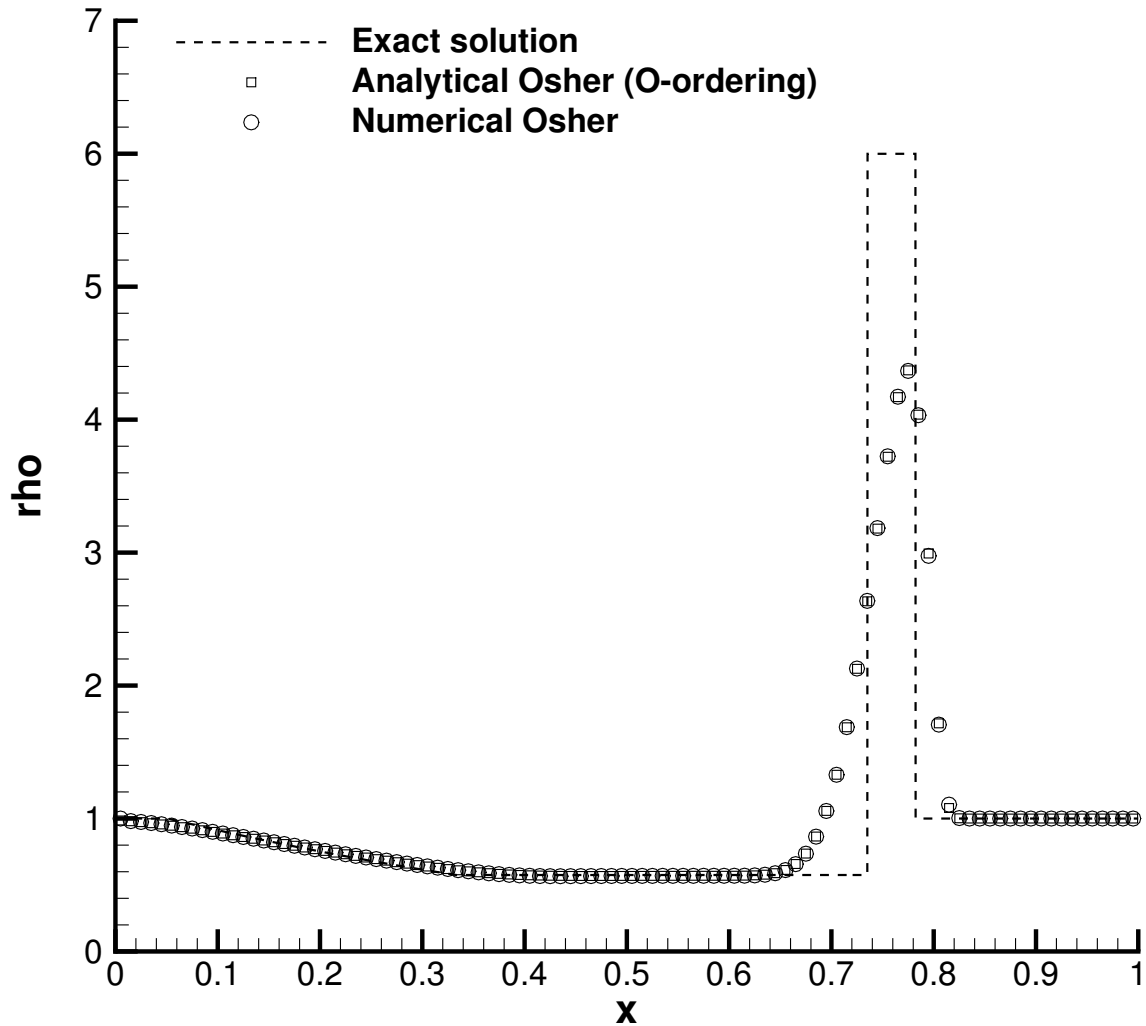

Euler equations: LHS of Wooodward-Colella test.

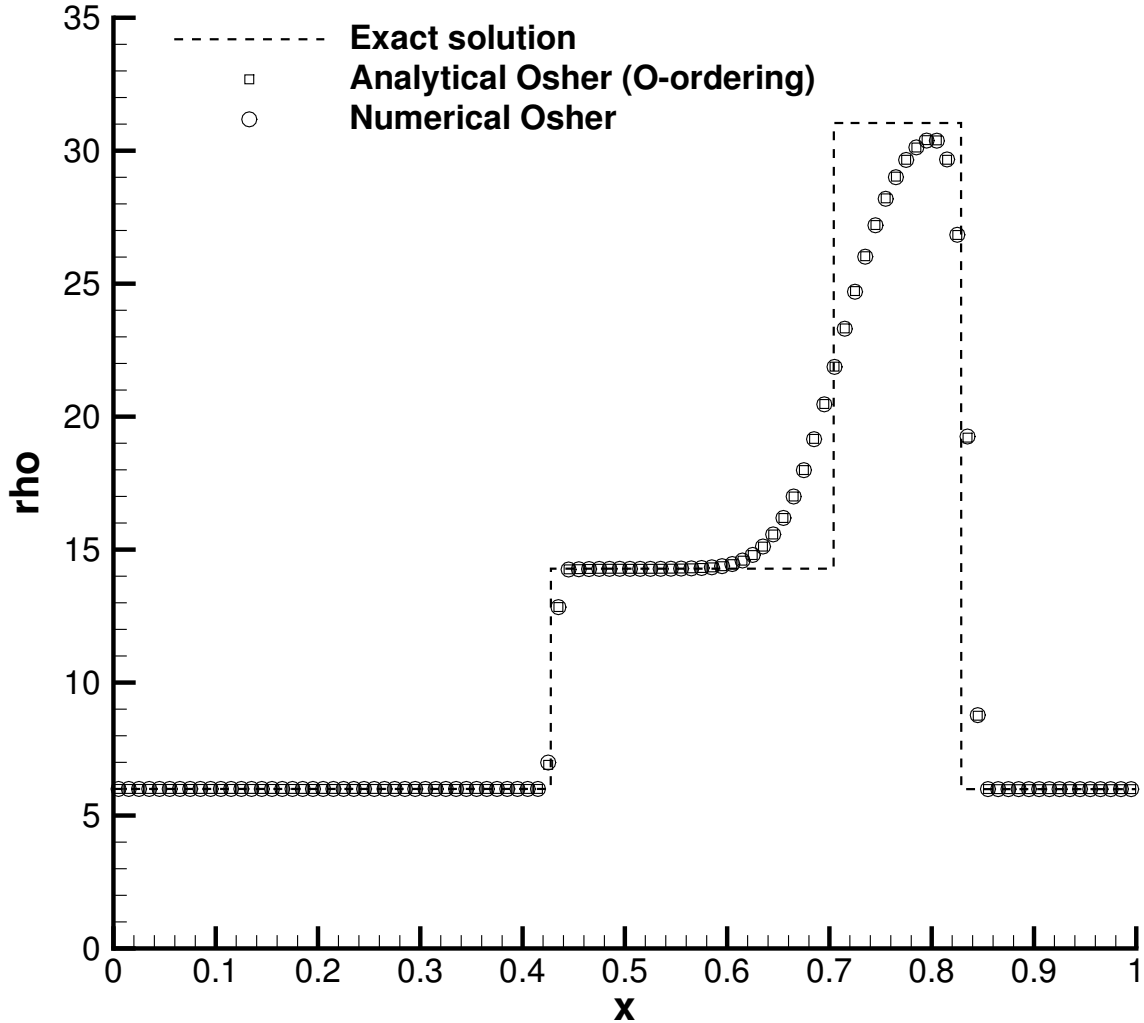

Euler equations: two-shock collision.

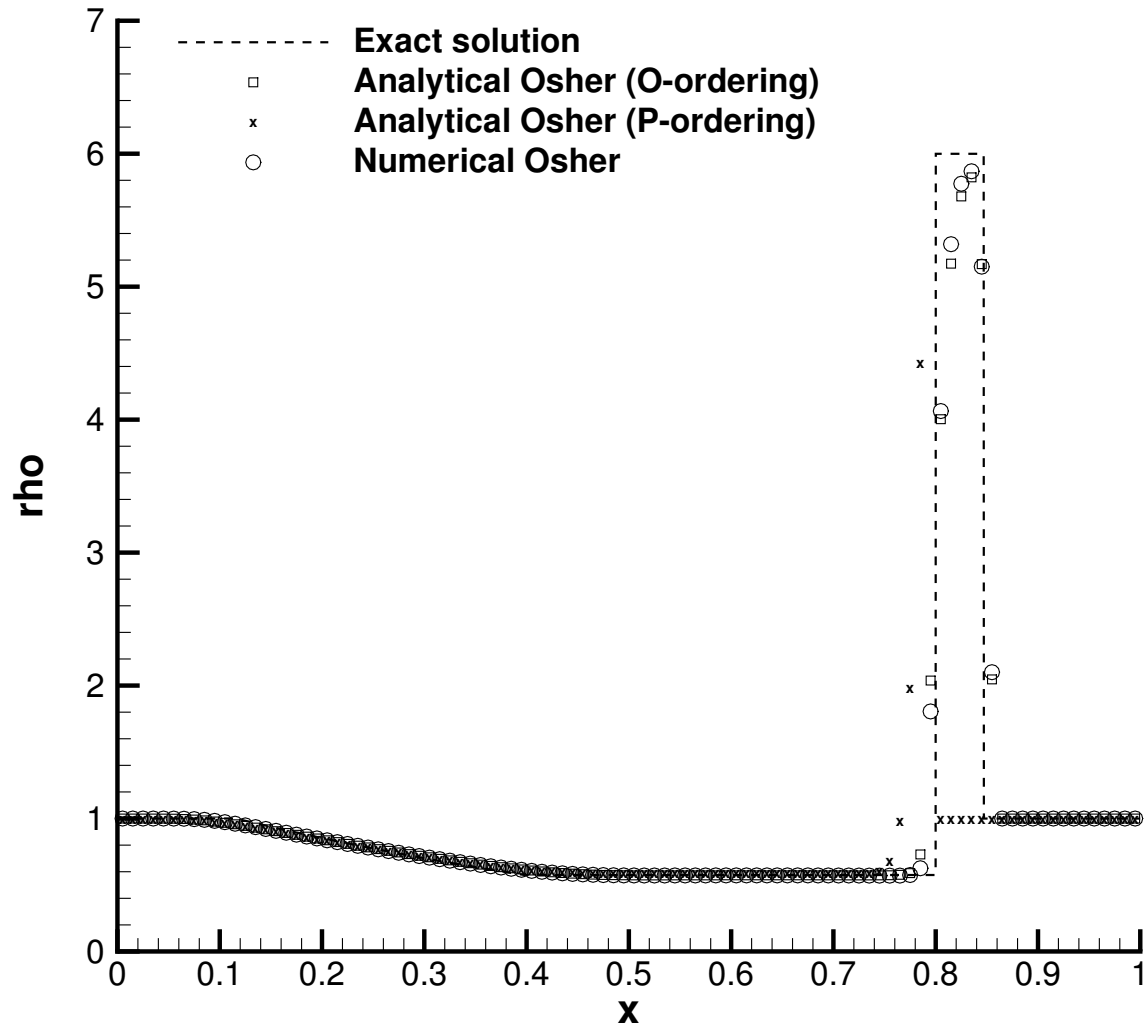

Euler equations: non-isolated stationary contact.

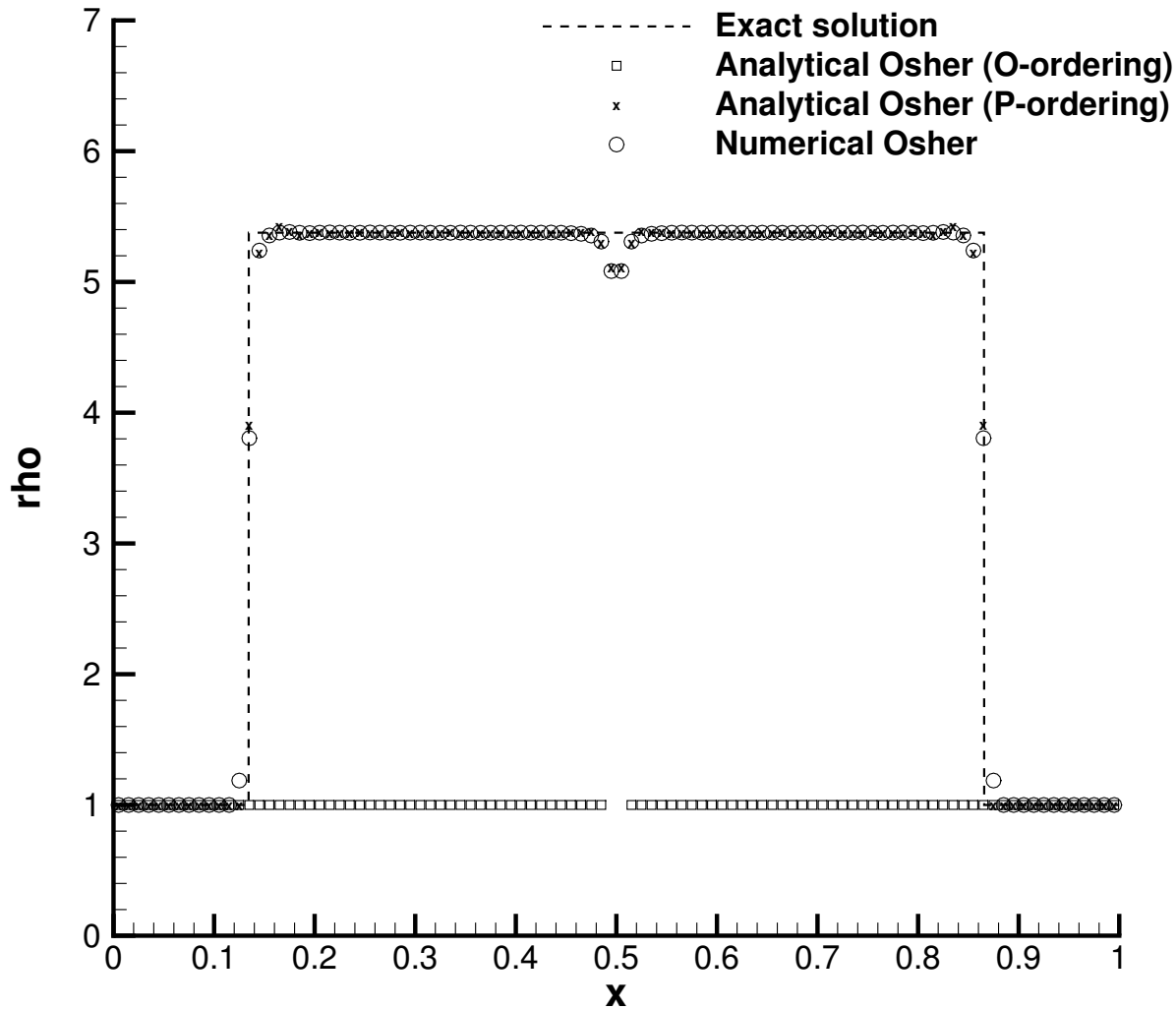

Euler equations: two-shock Riemann problem.

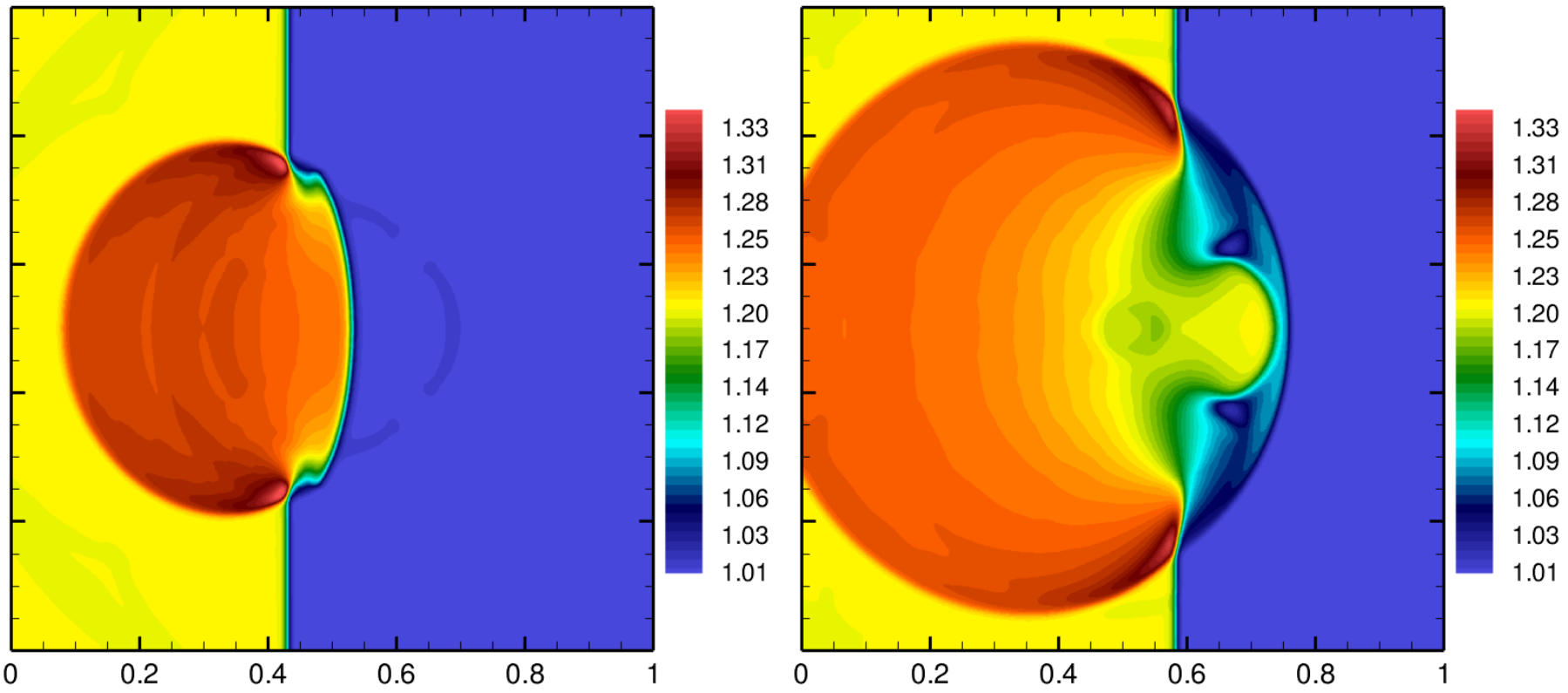

Euler equations with JWL EOS.
Shock-bubble interaction using conservative DOT:
pressure contours at $\tilde{t} = 0.25$ (left)
and $\tilde{t} = 0.35$ (right)

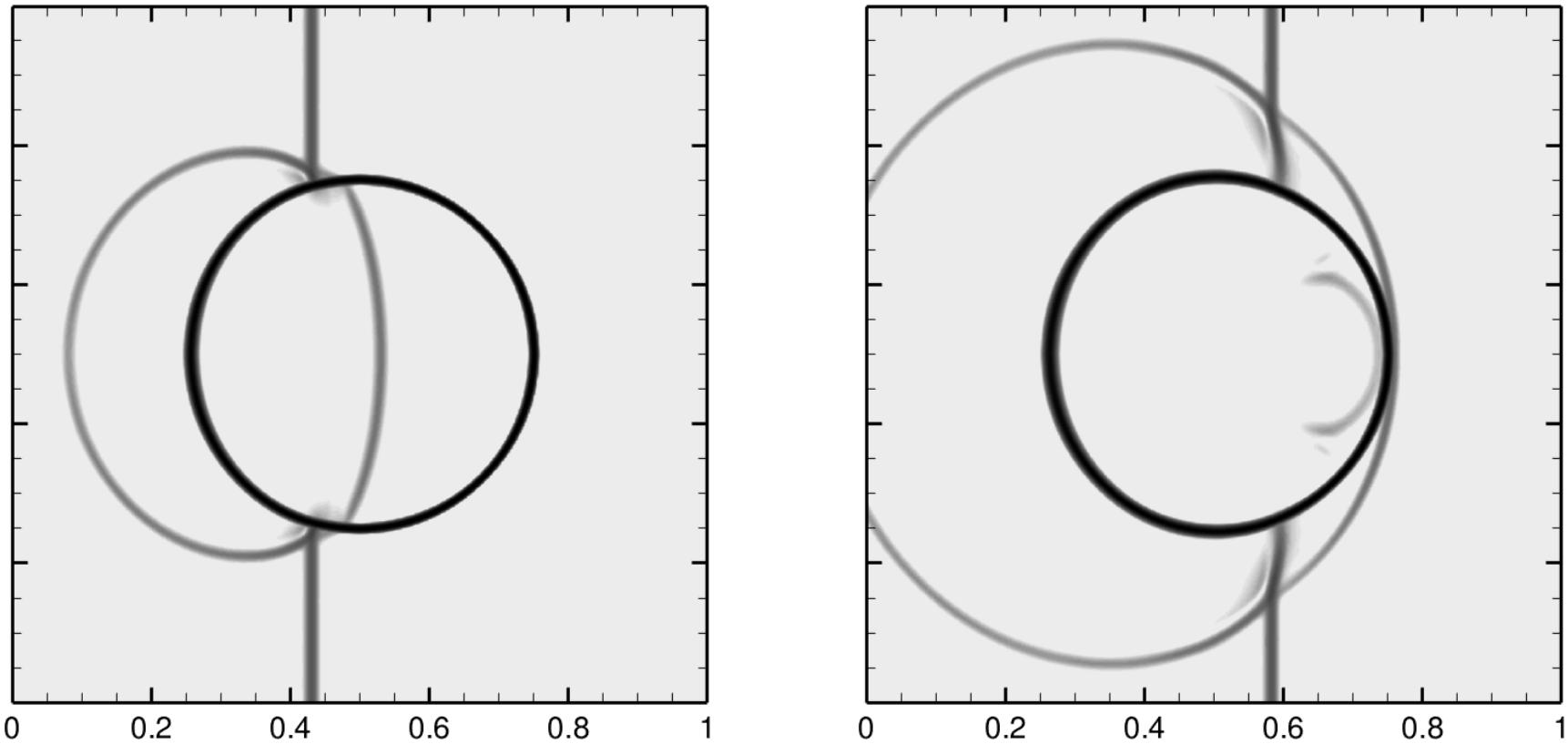

Euler equations with JWL EOS.
Shock-bubble interaction using conservative DOT:
numerical Schlieren at $\tilde{t} = 0.25$ (left)
and $\tilde{t} = 0.35$ (right)

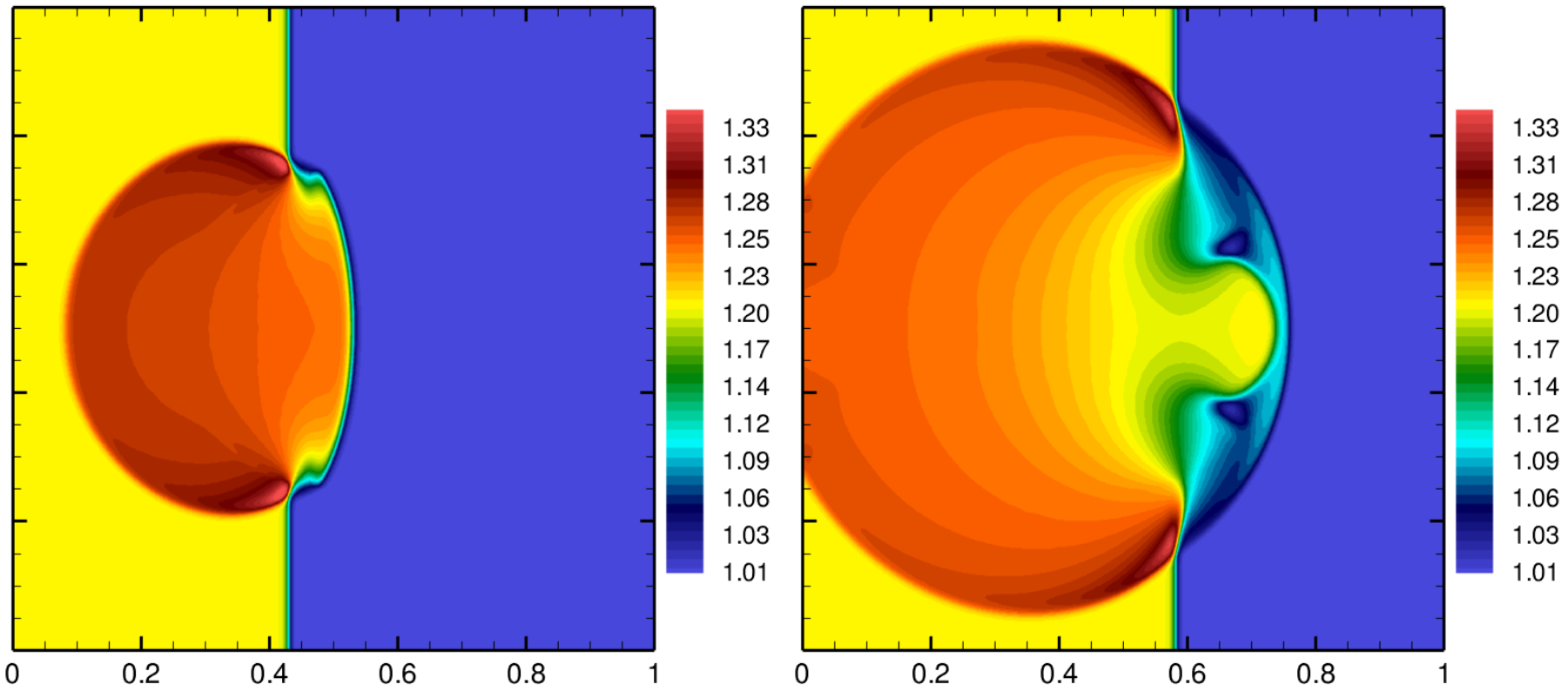

Euler equations with JWL EOS.
Shock-bubble interaction using adaptive DOT scheme:
numerical Schlieren at $\tilde{t} = 0.25$ (left) and $\tilde{t} = 0.35$ (right)

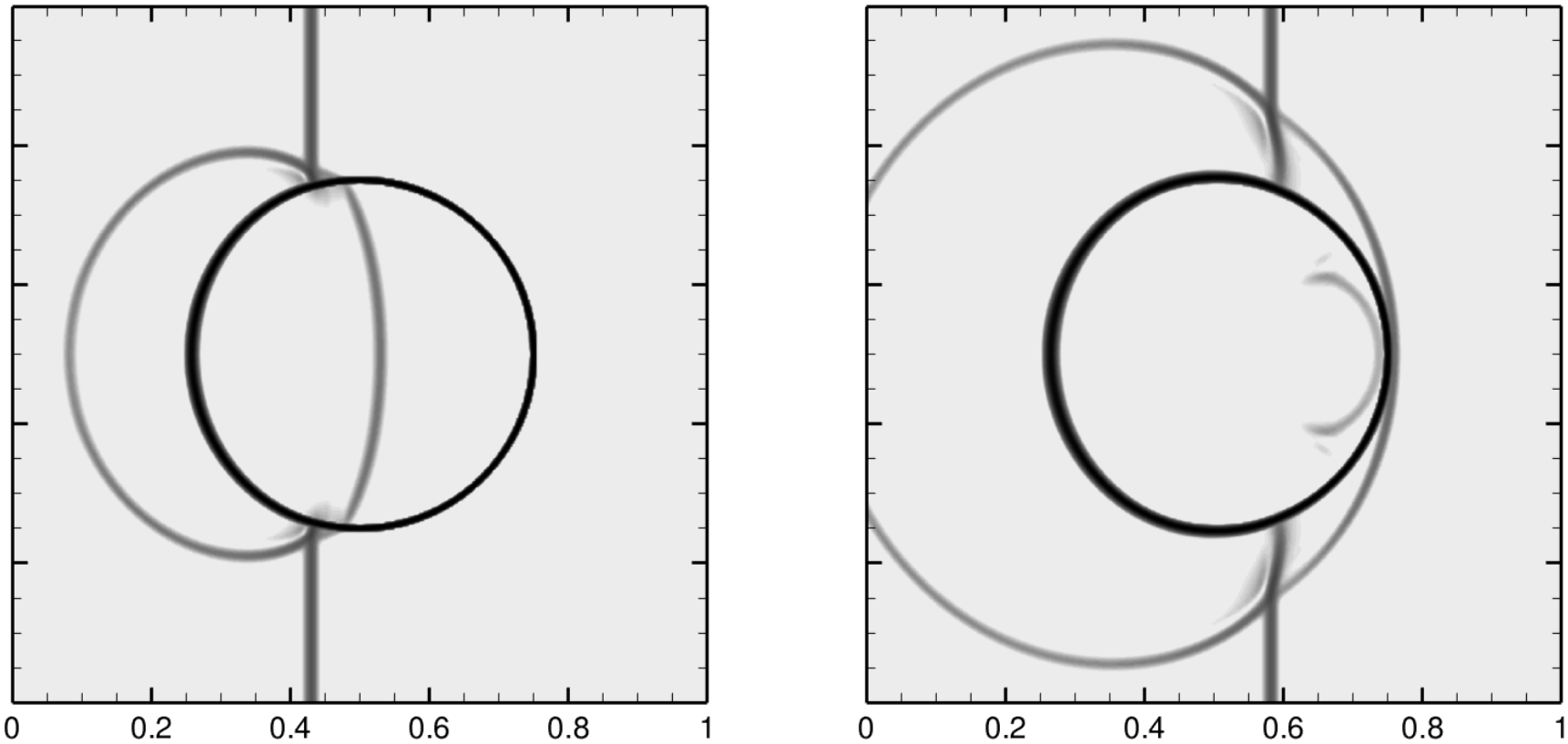

Euler equations with JWL EOS.
Shock-bubble interaction using adaptive DOT scheme: numerical Schlieren (upper) and pressure contours (lower), at $\tilde{t} = 0.25$ (left) and $\tilde{t} = 0.35$ (right)

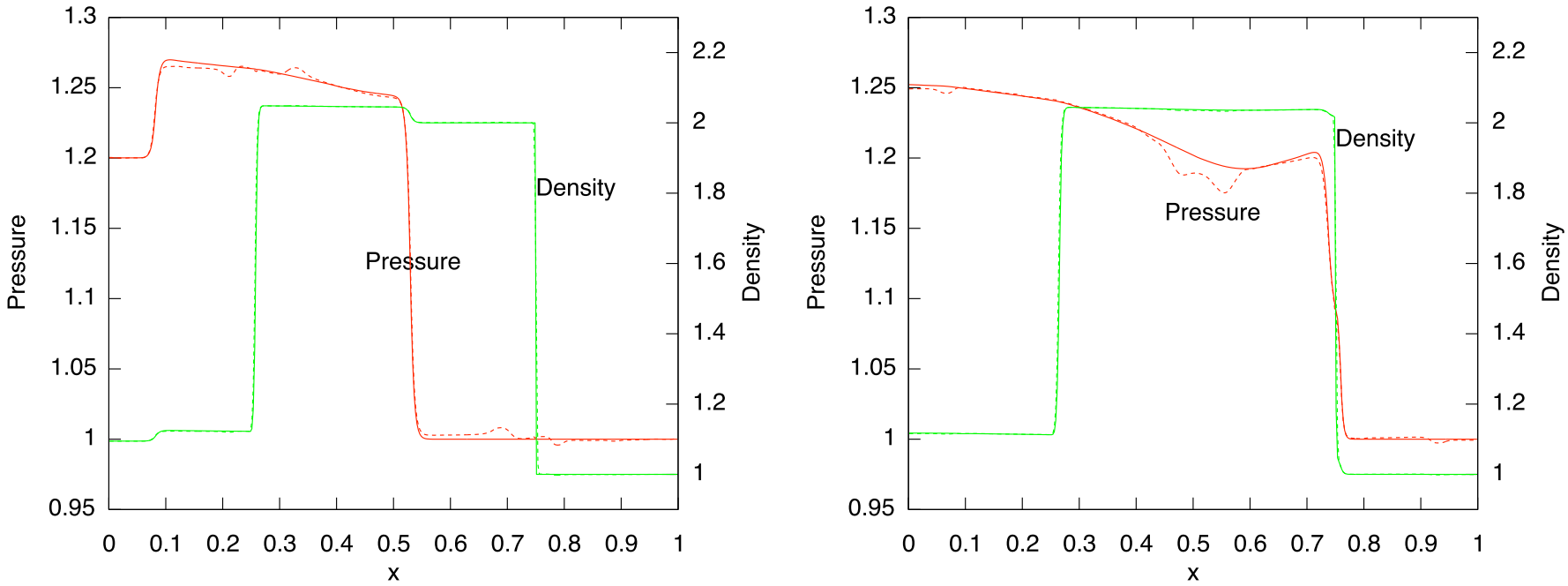

Euler equations with JWL EOS.
Pressure (red) and density (green) distribution along $\tilde{y} = 0.5$ of two-dimensional shock-bubble interaction using conservative DOT (dashed line) and adaptive DOT (solid line), at $\tilde{t} = 0.25$ (top) and $\tilde{t} = 0.35$ (bottom)

Part A: Concluding Remarks

- Generalized Osher-type scheme presented
- It is applicable to any hyperbolic system
- Scheme preserves good properties of original scheme
- Scheme resolves some difficulties of original scheme
- Applications include: Euler equations with general equations of state; two-phase flow; blood flow; shallow water flows, etc.

Part B:

New flux splitting schemes for the Euler equations

B1: The Euler Equations and Flux Splitting

The Euler equations in one space dimension are

$$\partial_t \mathbf{Q} + \partial_x \mathbf{F}(\mathbf{Q}) = \mathbf{0} \,, \tag{25}$$

where $\mathbf{Q}$ is the vector of conserved variables and $\mathbf{F}(\mathbf{Q})$ is the flux vector, both given as

$$\mathbf{Q} = \begin{bmatrix} \rho \\ \rho u \\ E \end{bmatrix} \,, \quad \mathbf{F}(\mathbf{Q}) = \begin{bmatrix} \rho u \\ \rho u^2 + p \\ u(E+p) \end{bmatrix} \,. \tag{26}$$

Here ρ is density, u is particle velocity, p is pressure and E is total energy given as

$$E = \rho(\frac{1}{2}u^2 + e) \,. \tag{27}$$

The specific internal energy e is, in general, a function of other variables via an equation of state. For example, e may be taken to be a function of density and pressure, namely

$$e = e(\rho, p) \,. \tag{28}$$

For ideal gases

$$e(\rho, p) = \frac{p}{\rho(\gamma - 1)} \,, \tag{29}$$

where $1 < \gamma < 3$ is the ratio of specific heats. For air at moderate pressures and temperatures one uses $\gamma = 1.4$.
For solving numerically equations of the type (25) we adopt a conservative method of the form

$$\mathbf{Q}_i^{n+1} = \mathbf{Q}_i^n - \frac{\Delta t}{\Delta x}[\mathbf{F}_{i+\frac{1}{2}} - \mathbf{F}_{i-\frac{1}{2}}] \,, \tag{30}$$

where $\mathbf{F}_{i+\frac{1}{2}}$ is the numerical flux. For background on the Euler equations and conservative schemes of the form (30).

Flux vector splitting:

$$\mathbf{F}(\mathbf{Q}) = \mathbf{A}(\mathbf{Q}) + \mathbf{P}(\mathbf{Q}) \,, \tag{31}$$

B2: The Liou-Steffen Splitting

Liou and Steffen (1993) split the flux vector into and advection part $\mathbf{A}(\mathbf{Q})$ and a pressure part $\mathbf{P}(\mathbf{Q})$ as follows

$$\mathbf{F}(\mathbf{Q}) = \mathbf{A}(\mathbf{Q}) + \mathbf{P}(\mathbf{Q}) \,,$$

with

$$\mathbf{A}(\mathbf{Q}) = \begin{bmatrix} \rho u \\ \rho u^2 \\ \rho u H \end{bmatrix} \,, \quad \mathbf{P}(\mathbf{Q}) = \begin{bmatrix} 0 \\ p \\ 0 \end{bmatrix} \,, \tag{32}$$

where

$$H = \frac{E + p}{\rho} \tag{33}$$

is the enthalpy.

From the numerical point of view the aim is to obtain a numerical flux for (30) of the form

$$\mathbf{F}_{i+\frac{1}{2}} = \mathbf{A}_{i+\frac{1}{2}} + \mathbf{P}_{i+\frac{1}{2}} \tag{34}$$

by finding *partial* advection and pressure fluxes $\mathbf{A}_{i+\frac{1}{2}}$ and $\mathbf{P}_{i+\frac{1}{2}}$.

Liou and Steffen express $\mathbf{A}(\mathbf{Q})$ as

$$\mathbf{A}(\mathbf{Q}) = M \begin{bmatrix} \rho a \\ \rho a u \\ \rho a H \end{bmatrix} , \tag{35}$$

where $M = u/a$ is the Mach number and $a = \sqrt{\gamma p/\rho}$ is the speed of sound. The advection flux is then taken as

$$\mathbf{A}_{i+\frac{1}{2}} = M_{i+\frac{1}{2}} \hat{\mathbf{A}}_{i+\frac{1}{2}} , \tag{36}$$

with

$$\hat{\mathbf{A}}_{i+\frac{1}{2}} = \begin{cases} \begin{bmatrix} \rho a \\ \rho a u \\ \rho a H \end{bmatrix}_i^n & \text{if} \quad M_{i+\frac{1}{2}} \geq 0 , \\ \\ \begin{bmatrix} \rho a \\ \rho a u \\ \rho a H \end{bmatrix}_{i+1}^n & \text{if} \quad M_{i+\frac{1}{2}} < 0 . \end{cases} \tag{37}$$

The advection flux is *upwinded* according to advection speed *implied* in the Mach number $M_{i+\frac{1}{2}}$, which is split as

$$M_{i+\frac{1}{2}} = M_i^+ + M_{i+1}^- \,, \tag{38}$$

with

$$M^{\pm} = \begin{cases} \pm\frac{1}{4}(M\pm 1)^2 & \text{if} \quad |\,M\,| \leq 1\,, \\ \frac{1}{2}(M\pm |\,M\,|) & \text{if} \quad |\,M\,| > 1\,. \end{cases} \tag{39}$$

The pressure vector $\mathbf{P}_{i+\frac{1}{2}}$ is constructed by splitting the pressure as

$$p_{i+\frac{1}{2}} = p_i^+ + p_{i+1}^- \,, \tag{40}$$

with two choices for the negative and positive components

$$p^{\pm} = \begin{cases} \frac{1}{2}p(1\pm M) & \text{if} \quad |\,M\,| \leq 1\,, \\ \frac{1}{2}p\frac{(M\pm|M|)}{M} & \text{if} \quad |\,M\,| > 1\,, \end{cases} \tag{41}$$

and

$$p^{\pm} = \begin{cases} \frac{1}{4}p(M\pm 1)^2(2\mp M) & \text{if} \quad |\,M\,| \leq 1\,, \\ \frac{1}{2}p\frac{(M\pm|M|)}{M} & \text{if} \quad |\,M\,| > 1\,. \end{cases} \tag{42}$$

B3: The Zha-Bilgen Splitting

Zha and Bilgen (1993) split the flux vector into as in (31) with

$$\mathbf{A}(\mathbf{Q}) = \begin{bmatrix} \rho u \\ \rho u^2 \\ uE \end{bmatrix} , \quad \mathbf{P}(\mathbf{Q}) = \begin{bmatrix} 0 \\ p \\ pu \end{bmatrix} . \tag{43}$$

Numerically, they propose fluxes $\mathbf{A}_{i+\frac{1}{2}}$ and $\mathbf{P}_{i+\frac{1}{2}}$ as follows.

$$\mathbf{A}_{i+\frac{1}{2}} = \mathbf{A}_i^+ + \mathbf{A}_{i+1}^- , \tag{44}$$

where

$$\mathbf{A}_i^- = min(0, u_i^n)\mathbf{Q}_i^n , \quad \mathbf{A}_i^+ = max(0, u_i^n)\mathbf{Q}_i^n . \tag{45}$$

For the pressure flux vector Zha and Bilgen use the splitting

$$\mathbf{P}_{i+\frac{1}{2}} = \mathbf{P}_i^+ + \mathbf{P}_{i+1}^- . \tag{46}$$

For the p component Zha and Bilgen adopt the Liou-Steffen splitting (40), (41), while for the pu component they propose

$$(pu)_{i+\frac{1}{2}} = (pu)_i^+ + (pu)_{i+1}^- \,, \tag{47}$$

where

$$(pu)_i^- = p_i^n \begin{cases} u_i^n & \text{if} \quad M_i^n \le -1 \,, \\ \frac{1}{2}(u_i^n - a_i^n) & \text{if} \quad -1 < M_i^n < 1 \,, \\ 0 & \text{if} \quad M_i^n \ge 1 \,, \end{cases} \tag{48}$$

and

$$(pu)_i^+ = p_i^n \begin{cases} 0 & \text{if} \quad M_i^n \le -1 \,, \\ \frac{1}{2}(u_i^n + a_i^n) & \text{if} \quad -1 < M_i^n < 1 \,, \\ u_i^n & \text{if} \quad M_i^n \ge 1 \,. \end{cases} \tag{49}$$

Finally the Zha-Bilgen numerical flux is

$$\mathbf{F}_{i+\frac{1}{2}} = \mathbf{A}_i^+ + \mathbf{P}_i^+ + \mathbf{A}_{i+1}^- + \mathbf{P}_{i+1}^- \,. \tag{50}$$

B4: A Flux-Splitting Framework

The framework.

We propose to split system (25) via the flux splitting (31) into the two systems

$$\left.\begin{aligned} \partial_t \mathbf{Q} + \partial_x \mathbf{A}(\mathbf{Q}) &= \mathbf{0} \,, \\ \partial_t \mathbf{Q} + \partial_x \mathbf{P}(\mathbf{Q}) &= \mathbf{0} \,, \end{aligned}\right\} \tag{51}$$

called respectively the *advection system* and the *pressure system*. The aim is then to compute a numerical flux as

$$\mathbf{F}_{i+\frac{1}{2}} = \mathbf{A}_{i+\frac{1}{2}} + \mathbf{P}_{i+\frac{1}{2}} \,, \tag{52}$$

where $\mathbf{A}_{i+\frac{1}{2}}$ and $\mathbf{P}_{i+\frac{1}{2}}$ are obtained respectively from appropriate Cauchy problems for the advection and pressure systems (51).

Consider the Cauchy problem for the linear advection equation

$$\left.\begin{array}{l} \partial_t q(x,t) + \lambda \partial_x q(x,t) = 0 \ , -\infty < x < \infty \ , \quad t > 0 \ , \\ q(x,0) = h(x) \ , \end{array}\right\} \tag{53}$$

where λ is a constant. The exact solution of IVP (53) after a time Δt is

$$q(x, \Delta t) = h(x - \lambda \Delta t) \ . \tag{54}$$

We now decompose the characteristic speed λ as

$$\lambda = \beta\lambda + (1-\beta)\lambda = \lambda_a + \lambda_p \ , \quad 0 \leq \beta \leq 1 \ , \tag{55}$$

with definitions

$$\lambda_a = \beta\lambda \ , \quad \lambda_p = (1-\beta)\lambda \ , \tag{56}$$

so as to obtain two linear partial differential equations, namely

$$\partial_t q + \lambda_a \partial_x q = 0 \ , \quad \partial_t q + \lambda_p \partial_x q = 0 \ . \tag{57}$$

Now consider first the Cauchy problem for the *advection* equation

$$\left.\begin{array}{l} \partial_t \tilde{q} + \lambda_a \partial_x \tilde{q} = 0 \ , \\ \tilde{q}(x,0) = h(x) \ , \end{array}\right\} \tag{58}$$

the solution of which after a time Δt_1 is

$$\tilde{q}(x, \Delta t_1) = h(x - \lambda_a \Delta t_1) \ . \tag{59}$$

Consider the Cauchy problem

$$\left.\begin{array}{l} \partial_t \bar{q} + \lambda_p \partial_x \bar{q} = 0 \ , \\ \bar{q}(x,0) = h(x - \lambda_a \Delta t_1) \ . \end{array}\right\} \tag{60}$$

The exact solution of IVP (60), after a time Δt_2, is

$$\bar{q}(x, \Delta t_2) = h(x - \lambda_a \Delta t_1 - \lambda_p \Delta t_2) \ . \tag{61}$$

The combined solution of IVPs (58) and (60) for $\Delta t_1 = \Delta t_2 = \Delta t$ is

$$\bar{q}(x, \Delta t) = h(x - (\lambda_a + \lambda_p)\Delta t) = h(x - \lambda \Delta t) = q(x, \Delta t) \ . \tag{62}$$

The above result can be stated as the following proposition.

Proposition 1. The exact solution of the initial value problem (53) can be obtained by solving in sequence the initial-value problems (58) and (60).

Remarks:

- In the wave decomposition (55),(56) of the model problem (53) the characteristic speeds to be arbitrarily different.
- From the numerical point of view, Proposition 1 suggests a way to compute a numerical flux for IVP (53) by computing numerical fluxes for IVPs (58) and (60). This would lead to *split* flux vector splitting methods and could potentially be of use to deal with systems in which there is large disparity in the magnitude of the wave speeds present.
- For the full non-linear problem the proposed framework has two components: (a) the particular way the full system is split into two subsystems and (b) the numerical treatment of each subsystem to produce corresponding advection and pressure numerical fluxes.

B5: A Novel Splitting for the Euler Equations

Here we propose a new splitting for the Euler equations by noting that the flux may be decomposed thus

$$\mathbf{F}(\mathbf{Q}) = \begin{bmatrix} \rho u \\ \rho u^2 + p \\ u(\frac{1}{2}\rho u^2 + \rho e + p) \end{bmatrix} = \begin{bmatrix} \rho u \\ \rho u^2 \\ \frac{1}{2}\rho u^3 \end{bmatrix} + \begin{bmatrix} 0 \\ p \\ u(\rho e + p) \end{bmatrix}, \tag{63}$$

with the corresponding advection and pressure fluxes defined as

$$\mathbf{A}(\mathbf{Q}) = u \begin{bmatrix} \rho \\ \rho u \\ \frac{1}{2}\rho u^2 \end{bmatrix}, \quad \mathbf{P}(\mathbf{Q}) = \begin{bmatrix} 0 \\ p \\ u(\rho e + p) \end{bmatrix}. \tag{64}$$

Remarks:

- The proposed advection flux $\mathbf{A}(\mathbf{Q})$ contains no pressure terms.
- All pressure terms from the flux $\mathbf{F}(\mathbf{Q})$, including that of the total energy E, are now included in the pressure flux $\mathbf{P}(\mathbf{Q})$.
- The advection flux may be interpreted as representing advection of mass, momentum and kinetic energy.
- For the ideal gas case (29) the pressure flux (64) becomes

$$\mathbf{P}(\mathbf{Q}) = \begin{bmatrix} 0 \\ p \\ \frac{\gamma}{\gamma-1} pu \end{bmatrix} . \tag{65}$$

The advection system is

$$\partial_t \mathbf{Q} + \partial_x \mathbf{A}(\mathbf{Q}) = \mathbf{0}\,, \tag{66}$$

where $\mathbf{Q} = [\rho, \rho u, E]^T$ and $\mathbf{A}(\mathbf{Q})$ as in (64) above. In quasi-linear form the advection system becomes

$$\partial_t \mathbf{Q} + \mathbf{M}(\mathbf{Q})\partial_x \mathbf{Q} = \mathbf{0}\,, \tag{67}$$

where $\mathbf{M}(\mathbf{Q})$ is the Jacobian matrix given as

$$\mathbf{M}(\mathbf{Q}) = \begin{bmatrix} 0 & 0 & 0 \\ -u^2 & 2u & 0 \\ -u^3 & \frac{3}{2}u^2 & 0 \end{bmatrix}\,. \tag{68}$$

It is easy to show that the eigenvalues of this matrix are

$$\lambda_1 = 0\,, \quad \lambda_2 = \lambda_3 = u\,. \tag{69}$$

There are only two linearly independent right eigenvectors, namely

$$\mathbf{R_1} = \alpha_1 \begin{bmatrix} 1 \\ 0 \\ 0 \end{bmatrix}\,, \; \mathbf{R_2} = \alpha_2 \begin{bmatrix} 1 \\ u \\ \frac{1}{2}u^2 \end{bmatrix}\,. \tag{70}$$

Thus the system is *weakly hyperbolic*, as there is no complete set of linearly independent eigenvectors.

Regarding the nature of the characteristic fields, it is easy to show that the λ_1-field is linearly degenerated and that the λ_2-field is genuinely non-linear if $\alpha_2 \neq 0$ and $u \neq 0$; otherwise it is linearly degenerate.

The pressure system.

In terms of the conserved variables $\mathbf{Q} = [\rho, \rho u, E]^T$ the pressure system is

$$\partial_t \mathbf{Q} + \partial_x \mathbf{P}(\mathbf{Q}) = \mathbf{0} \,, \tag{71}$$

with $\mathbf{P}(\mathbf{Q})$ as given in (64) above. In quasi-linear form the advection system becomes

$$\partial_t \mathbf{Q} + \mathbf{N}(\mathbf{Q}) \partial_x \mathbf{Q} = \mathbf{0} \,, \tag{72}$$

where $\mathbf{N}(\mathbf{Q})$ is the Jacobian matrix given as

$$\mathbf{N}(\mathbf{Q}) = \begin{bmatrix} 0 & 0 & 0 \\ \frac{1}{2}(\gamma-1)u^2 & -(\gamma-1)u & \gamma-1 \\ \gamma u^3 - \gamma u E/\rho & \gamma E/\rho - \frac{3}{2}\gamma u^2 & \gamma u \end{bmatrix} . \tag{73}$$

The eigenvalues of $\mathbf{N}(\mathbf{Q})$ are always real and given as

$$\lambda_1 = \frac{1}{2}u - \frac{1}{2}A\,, \quad \lambda_2 = 0\,, \quad \lambda_3 = \frac{1}{2}u + \frac{1}{2}A\,, \tag{74}$$

where

$$A = \sqrt{u^2 + 4a^2}\,, \quad a^2 = \frac{\gamma p}{\rho}\,. \tag{75}$$

Here a is the usual speed of sound for the full Euler equations. In terms of physical variables the system reads

$$\partial_t \mathbf{V} + \mathbf{B}(\mathbf{V})\partial_x \mathbf{V} = \mathbf{0}\,, \tag{76}$$

where

$$\mathbf{V} = \begin{bmatrix} \rho \\ u \\ p \end{bmatrix}\,, \quad \mathbf{B} = \begin{bmatrix} 0 & 0 & 0 \\ 0 & 0 & 1/\rho \\ 0 & \gamma p & u \end{bmatrix}\,. \tag{77}$$

Note that, since $u < A = \sqrt{u^2 + 4a^2}$, the system is *always subsonic*, that is

$$\lambda_1 = \frac{1}{2}u - \frac{1}{2}A < 0 < \lambda_3 = \frac{1}{2}u + \frac{1}{2}A \,. \tag{78}$$

The right eigenvectors of matrix $\mathbf{B}$ in (77) corresponding to the eigenvalues (74) are

$$\mathbf{R_1} = \begin{bmatrix} 0 \\ 2 \\ \rho(u - A) \end{bmatrix} , \; \mathbf{R_2} = \begin{bmatrix} 1 \\ 0 \\ 0 \end{bmatrix} , \; \mathbf{R_3} = \begin{bmatrix} 0 \\ 2 \\ \rho(u + A) \end{bmatrix} . \tag{79}$$

B6: Numerical Fluxes for Toro-Vázquez splitting

In order to compute advection and pressure fluxes $\mathbf{A}_{i+\frac{1}{2}}$ and $\mathbf{P}_{i+\frac{1}{2}}$ we consider the Riemann problem for each subsystem. We start with the pressure system.

To compute the flux for the pressure system we consider the Riemann problem in terms of physical variables

$$\left.\begin{aligned} &\partial_t \mathbf{V} + \mathbf{B}(\mathbf{V})\partial_x \mathbf{V} = \mathbf{0}\,, \\ &\mathbf{V}(x,0) = \begin{cases} \mathbf{V}_L \equiv \mathbf{V}_i^n & \text{if} \quad x < 0\,, \\ \mathbf{V}_R \equiv \mathbf{V}_{i+1}^n & \text{if} \quad x > 0\,. \end{cases} \end{aligned}\right\} \tag{80}$$

The solution of this problem has structure as shown in Fig. B1. The wave pattern is always subsonic, with a stationary contact discontinuity and two non-linear waves to the left and right of the contact wave.

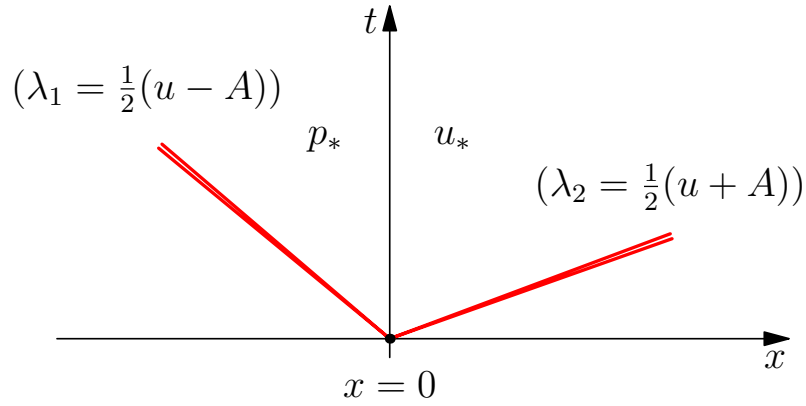

Fig. B1. Structure of the solution of the Riemann problem for the pressure system.

$$\left.\begin{aligned} u_* &= \frac{C_R u_R - C_L u_L}{C_R - C_L} - \frac{2}{C_R - C_L}(p_R - p_L) \ , \\ p_* &= \frac{C_R p_L - C_L p_R}{C_R - C_L} + \frac{1}{2}\frac{C_R C_L}{C_R - C_L}(u_R - u_L) \ , \end{aligned}\right\} \tag{81}$$

with

$$C_L = \rho_L(u_L - A_L) \ ; \quad C_R = \rho_R(u_R + A_R) \ , \tag{82}$$

where A_L and A_R are computed from (75).

One could improve upon the linear approximation by applying the exact generalised Riemann invariants throughout. The result is the 2×2 non-linear system for p_* and u_*

$$\left.\begin{aligned} u_* - \sqrt{u_*^2 + 4\frac{\gamma p_*}{\rho_L}} &= u_L - \sqrt{u_L^2 + 4\frac{\gamma p_L}{\rho_L}}\ , \\ u_* + \sqrt{u_*^2 + 4\frac{\gamma p_*}{\rho_R}} &= u_L + \sqrt{u_R^2 + 4\frac{\gamma p_R}{\rho_R}}\ . \end{aligned}\right\} \tag{83}$$

Finally, the numerical flux for the pressure system is given as

$$\mathbf{P}_{i+\frac{1}{2}} = p_* \begin{bmatrix} 0 \\ 1 \\ \frac{\gamma}{\gamma-1} u_* \end{bmatrix}\ . \tag{84}$$

Remark: no visible difference between "exact" and approximate solutions.

The advection system.

Recall that in our splitting (64) the advection operator may be written thus

$$\mathbf{A}(\mathbf{Q}) = \begin{bmatrix} \rho u \\ \rho u^2 \\ \frac{1}{2}\rho u^3 \end{bmatrix} = u\mathbf{K}(\mathbf{Q}) \,, \quad \mathbf{K}(\mathbf{Q}) = \begin{bmatrix} \rho \\ \rho u \\ \frac{1}{2}\rho u^2 \end{bmatrix} \,, \qquad (85)$$

Advection of $\mathbf{K}$ (mass, momentum and kinetic energy) with speed u. Here we propose two algorithms.

Algorith 1 (Toro-Vázquez scheme).

$$\mathbf{A}(\mathbf{Q}) = u^*_{i+\frac{1}{2}}\mathbf{K} \,, \qquad (86)$$

where $u^*_{i+\frac{1}{2}}$ is the intercell advection velocity taken as $u^*_{i+\frac{1}{2}}$ from solution (81) of the Riemann problem (80)

$$\mathbf{A}_{i+\frac{1}{2}} = u^*_{i+\frac{1}{2}} \begin{cases} \mathbf{K}^n_i & \text{if} \quad u^*_{i+\frac{1}{2}} > 0 \,, \\ \\ \mathbf{K}^n_{i+1} & \text{if} \quad u^*_{i+\frac{1}{2}} \leq 0 \,. \end{cases} \qquad (87)$$

Algorith 2 (TV-AWS scheme). We propose a weighted splitting scheme, a simple modification of the Zha-Bilgen scheme (1993):

$$\mathbf{A}_{i+\frac{1}{2}} = \mathbf{A}_i^+ + \mathbf{A}_{i+1}^- \,, \tag{88}$$

with

$$\mathbf{A}_i^- = \frac{1}{2}(1-\omega)u_i^n\mathbf{K}_i^n \,, \quad \mathbf{A}_i^+ = \frac{1}{2}(1+\omega)u_i^n\mathbf{K}_i^n \,. \tag{89}$$

Here

$$\omega = \omega(u_i^n) = \frac{u_i^n}{\sqrt{\epsilon + (u_i^n)^2}} \,, \tag{90}$$

with ϵ a small positive number, $\epsilon = 0.1$, for example.
The function $\omega(u_i^n)$ allows a smooth transition from upwinding fully to the left and fully to the right, in the vicinity of $u_i^n = 0$.
The TV-AWS scheme is a weighted averaged scheme and the Zha-Bilgen scheme, which is recovered by simply setting the weight to be $\omega = sign(u_i^n)$.

Summary of the Toro-Vázquez scheme.

In order to compute a numerical flux $\mathbf{F}_{i+\frac{1}{2}}$ for the conservative scheme (30) we proceed as follows:

- **Pressure flux.** Evaluate the intercell pressure $p^*_{i+\frac{1}{2}}$ and velocity $u^*_{i+\frac{1}{2}}$ from the solution of the Riemann problem given in (81) to compute the pressure flux $\mathbf{P}_{i+\frac{1}{2}}$ as in (84).
- **Advection flux.** We have proposed two options. From algorithm 1 (TV scheme) we evaluate the advection flux $\mathbf{A}_{i+\frac{1}{2}}$ as in (87). Algorith 2 (TV-AWS) is described in equations (88) to (90).
- **Intercell flux.** Compute the intercell flux $\mathbf{F}_{i+\frac{1}{2}}$ as in (52), namely

$$\mathbf{F}_{i+\frac{1}{2}} = \mathbf{A}_{i+\frac{1}{2}} + \mathbf{P}_{i+\frac{1}{2}} \ . \tag{91}$$

B7: Reinterpretation of Other Flux Splittings

The Liou-Steffen scheme

The Liou-Steffen splitting (1993) may be interpreted in our framework defining the advection system as

$$\partial_t \mathbf{Q} + \partial_x \mathbf{A}(\mathbf{Q}) = \mathbf{0}\,, \tag{92}$$

with

$$\mathbf{A}(\mathbf{Q}) = \begin{bmatrix} \rho u \\ \rho u^2 \\ u(E+p) \end{bmatrix} \tag{93}$$

and the pressure system as

$$\partial_t \mathbf{Q} + \partial_x \mathbf{P}(\mathbf{Q}) = \mathbf{0}\,, \tag{94}$$

with

$$\mathbf{P}(\mathbf{Q}) = \begin{bmatrix} 0 \\ p \\ 0 \end{bmatrix}\,. \tag{95}$$

In terms of primitive variables $\mathbf{V} = [\rho, u, p]^T$ the pressure system can be shown to hyperbolic with eigenvalues

$$\lambda_1 = \lambda_2 = 0\,, \quad \lambda_3 = -(\gamma - 1)u \tag{96}$$

and three linearly independent eigenvectors

$$\mathbf{R}_1 = \alpha_1 \begin{bmatrix} 1 \\ 0 \\ 0 \end{bmatrix}\,,\ \mathbf{R}_2 = \alpha_2 \begin{bmatrix} 0 \\ 1 \\ 0 \end{bmatrix}\,,\ \mathbf{R}_3 = \alpha_3 \begin{bmatrix} 0 \\ 1 \\ -\rho(\gamma - 1)u \end{bmatrix}\,. \tag{97}$$

Here α_1, α_2 and α_3 are scaling factors. Simple calculations show that the characteristic fields associated with λ_1 and λ_2 are *linearly degenerate* and the characteristic field associated with λ_3 is *genuinely non-linear*.

Unfortunately we have not been able to find a straightforward pressure numerical flux by solving the Riemann problem for this unusual hyperbolic system. Thus the re-interpretation of the Liou-Steffen splitting in our framework has not been productive.

The Zha-Bilgen splitting

The Zha-Bilgen splitting (1993) assumes a very natural splitting that may be interpreted in our framework as follows. The advection system is

$$\partial_t \mathbf{Q} + \partial_x \mathbf{A}(\mathbf{Q}) = \mathbf{0}\,, \quad \mathbf{A}(\mathbf{Q}) = \begin{bmatrix} \rho u \\ \rho u^2 \\ uE \end{bmatrix} \tag{98}$$

and the pressure system is

$$\partial_t \mathbf{Q} + \partial_x \mathbf{P}(\mathbf{Q}) = \mathbf{0}\,, \quad \mathbf{P}(\mathbf{Q}) = \begin{bmatrix} 0 \\ p \\ pu \end{bmatrix}\,. \tag{99}$$

In terms of primitive variables $\mathbf{V} = [\rho, u, p]^T$ the pressure system can be shown to be hyperbolic with real eigenvalues

$$\lambda_1 = -C\,, \quad \lambda_2 = 0\,, \quad \lambda_3 = C\,, \tag{100}$$

with

$$C = \sqrt{(\gamma - 1)p/\rho}\,, \tag{101}$$

and three linearly independent right eigenvectors

$$\mathbf{R}_1 = \alpha_1 \begin{bmatrix} 0 \\ 1 \\ -\rho C \end{bmatrix}\,, \; \mathbf{R}_2 = \alpha_2 \begin{bmatrix} 1 \\ 0 \\ 0 \end{bmatrix}\,, \; \mathbf{R}_3 = \alpha_3 \begin{bmatrix} 0 \\ 1 \\ \rho C \end{bmatrix}\,. \tag{102}$$

Here α_1, α_2 and α_3 are scaling factors.

The Riemann problem for the Zha-Bilgen pressure system in terms of primitive variables is

$$\left.\begin{aligned} &\partial_t \mathbf{V} + \mathbf{Z}(\mathbf{V})\partial_x \mathbf{V} = \mathbf{0} \\ &\mathbf{V}(x,0) = \begin{cases} \mathbf{V}_L \equiv \mathbf{V}_i^n & \text{if} \quad x < 0\,, \\ \mathbf{V}_R \equiv \mathbf{V}_{i+1}^n & \text{if} \quad x > 0\,. \end{cases} \end{aligned}\right\} \tag{103}$$

The structure of the solution is analogous to that shown in Fig. 1,

$$\left.\begin{aligned} u_* &= \frac{\rho_L C_L u_L + \rho_R C_R u_R}{\rho_L C_L + \rho_R C_R} - \frac{(p_R - p_L)}{\rho_L C_L + \rho_R C_R}\,, \\ p_* &= \frac{\rho_R C_R p_L + \rho_L C_L p_R}{\rho_L C_L + \rho_R C_R} - \frac{\rho_L C_L \rho_R C_R}{\rho_L C_L + \rho_R C_R}(u_R - u_L)\,, \end{aligned}\right\} \tag{104}$$

with

$$C_L = \sqrt{(\gamma - 1)p_L/\rho_L}\,, \quad C_R = \sqrt{(\gamma - 1)p_R/\rho_R}\,. \tag{105}$$

Contact Discontinuity.

Proposition 1. The Zha-Bilgen splitting along with the Zha-Bilgen numerical scheme cannot sustain isolated stationary contact discontinuities for the Euler equations.

Proof. Define the problem for a stationary, isolated contact discontinuity for the ideal gas Euler equations with initial condition

$$\left.\begin{array}{l} u(x,0)=0\ , \quad p(x,0)=\hat{p}: \text{constant}\ , \forall x \text{ such that } x_L<x<x_R\ , \\ \\ \rho(x,0)=\left\{\begin{array}{ll} \rho_L & \text{if} \quad x<x_0\ , \\ \\ \rho_R & \text{if} \quad x>x_0\ , \end{array}\right. \end{array}\right\} \tag{106}$$

with $x_L < x_0 < x_R$. Assume the discretisation of $[x_L, x_R]$ such that the contact discontinuity is between cells i and $i+1$. Application of the Zha-Bilgen scheme to any cell away from cells i and $i+1$ leaves the flow undisturbed.

However, application of the scheme to cell i for one time step gives

$$E_i^{n+1} = \frac{\hat{p}}{\gamma - 1} + \delta_i \hat{p} \ , \quad \delta_i = \frac{1}{2}\frac{\Delta t}{\Delta x}\sqrt{\gamma \hat{p}}\left(\frac{1}{\sqrt{\rho_R}} - \frac{1}{\sqrt{\rho_L}}\right) . \tag{107}$$

Application of the scheme to cell $i+1$ gives an analogous expression but with $\delta_{i+1} = -\delta_i$. In order to preserve the contact discontinuity unaltered one requires $\delta_i = 0$, which is not satisfied by the Zha-Bilgen scheme, as seen in (107).

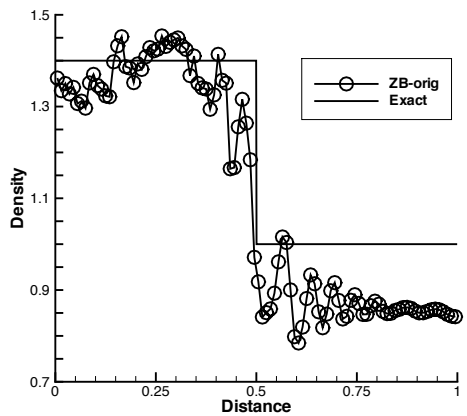

Fig. 2. Test 6: Stationary isolated contact. Exact (line) and numerical solution (symbols) using the Zha-Bilgen original scheme (ZB-orig).

Proposition 2. The Toro-Vázquez splitting (TV) along with their numerical method can recognise exactly isolated stationary contact discontinuities for the Euler equations.

Proof. Define the problem for a stationary, isolated contact discontinuity for the ideal gas Euler equations with initial condition as in (106). Assume the discretization of the domain $[x_L, x_R]$ is such that the cell just to the left of the discontinuity is i and that immediately to the right of the discontinuity is $i+1$. Application of the TV scheme to any cell away from cells i and $i+1$ leaves the flow indisturbed. Let us now apply the scheme to cell i for one time step. First we need the solution (81) of the Riemann problem with initial data (106). Clearly $u_* = u_{i+\frac{1}{2}} = 0$ and $p_* = p_{i+\frac{1}{2}} = \hat{p}$. Then it is easy to verify that the state $\mathbf{Q}_i^{n+1} = \mathbf{Q}_i^n$ and thus the isolated stationary contact is preserved exactly. Application of the scheme to cell $i+1$ gives an analogous result and the proposition is thus proved.

Proposition 3. The Zha-Bilgen splitting along with the Godunov-type numerical method of section 4.2 can recognise exactly isolated stationary contact discontinuities for the Euler equations.

Proof. The proof is straightforward and is thus omitted.

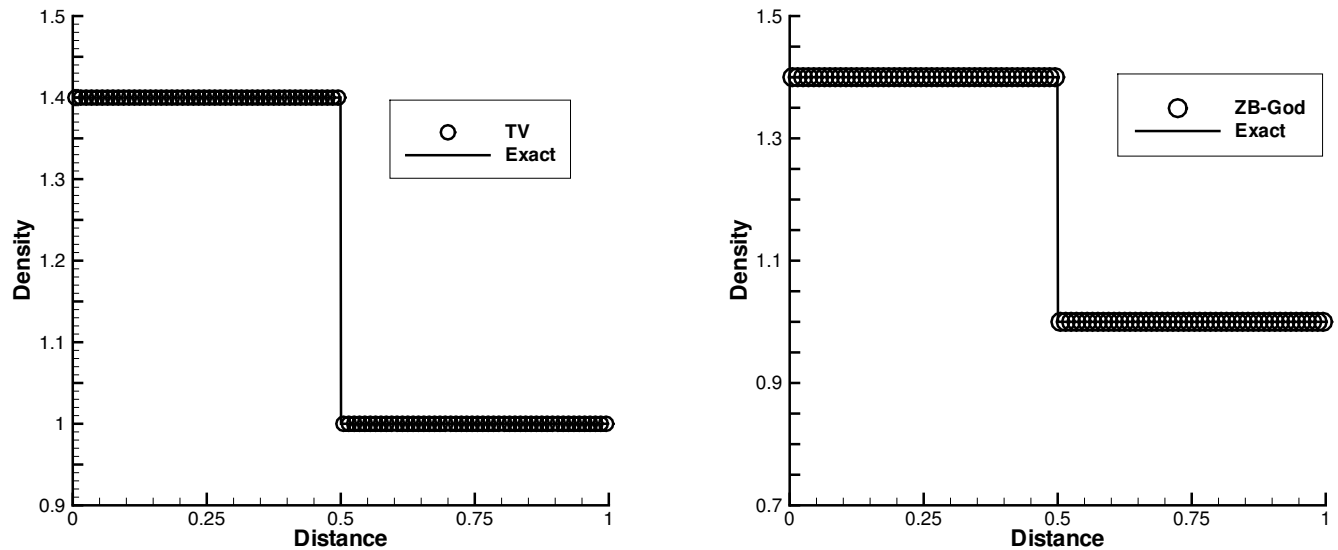

Fig. 3. Test 6: Stationary isolated contact. Exact (line) and numerical solutions (symbols).

B8: Numerical Results for the Euler Equations

Two classes of test problems

Test	ρ_{L}	u_{L}	p_{L}	ρ_{R}	u_{R}	p_{R}
1	1.0	0.75	1.0	0.125	0.0	0.1
2	1.0	-2.0	0.4	1.0	2.0	0.4
3	1.0	0.0	1000.0	1.0	0.0	0.01
4	5.99924	19.5975	460.894	5.99242	-6.19633	46.0950
5	1.0	-19.59745	1000.0	1.0	-19.59745	0.01
6	1.4	0.0	1.0	1.0	0.0	1.0

Test problems with exact solution (Toro, 2009)

Test of Woodward and Colella (1984). Reference solution: WAF.

$$\left.\begin{array}{lll} 0 \leq x \leq 0.1 & 0.1 < x \leq 0.9 & 0.9 < x \leq 1.0 \\ \rho_L = 1.0 & \rho_M = 1.0 & \rho_R = 1.0 \\ u_L = 0.0 & u_M = 0.0 & u_R = 0.0 \\ p_R = 1000.0 & p_M = 0.01 & p_R = 100.0 \end{array}\right\} \tag{108}$$

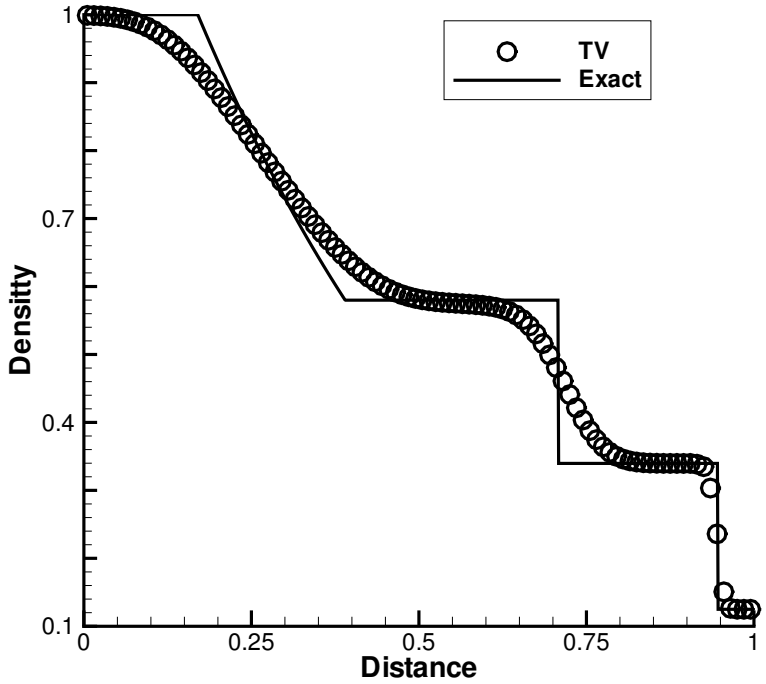

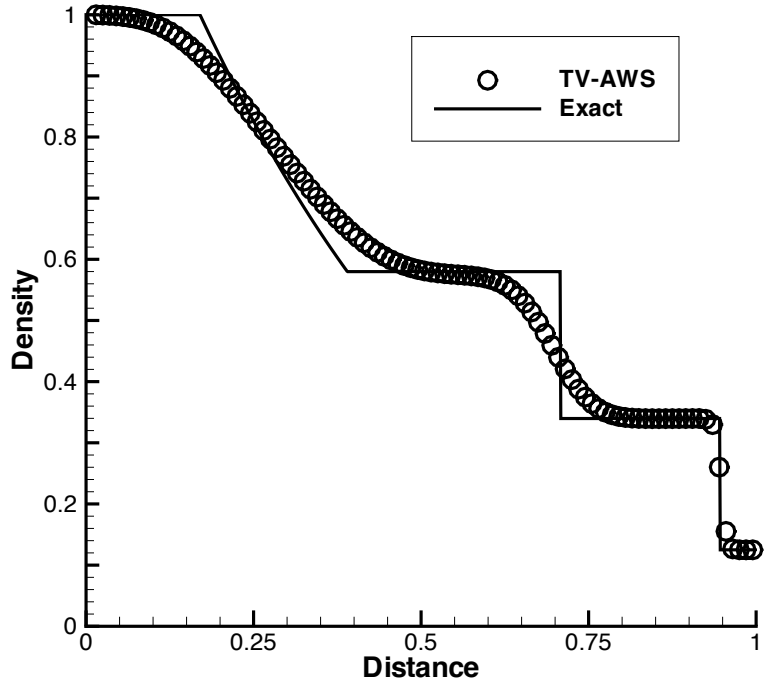

Test 1 (sonic flow). Exact (line) and numerical solutions (symbols) using two numerical schemes (TV and TV-AWS) for the flux splitting of this paper.

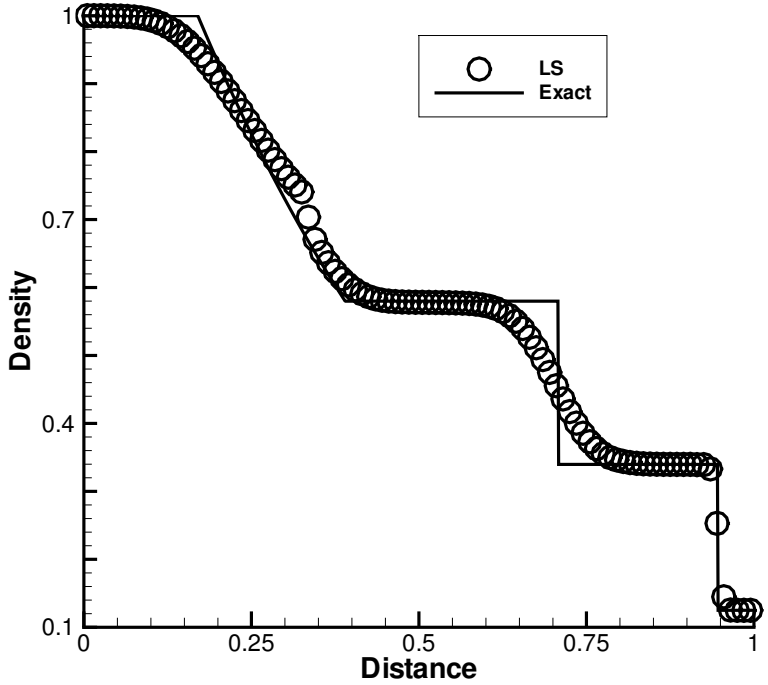

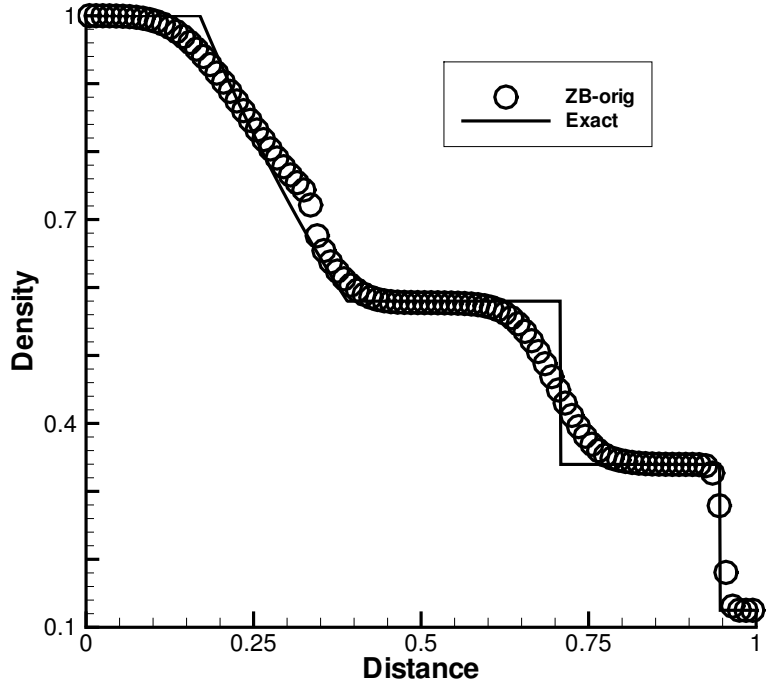

Test 1 (sonic flow). Exact (line) and numerical solutions (symbols) using two numerical schemes: Liou-Steffen (LS) and Zha-Bilgen (ZB-orig).

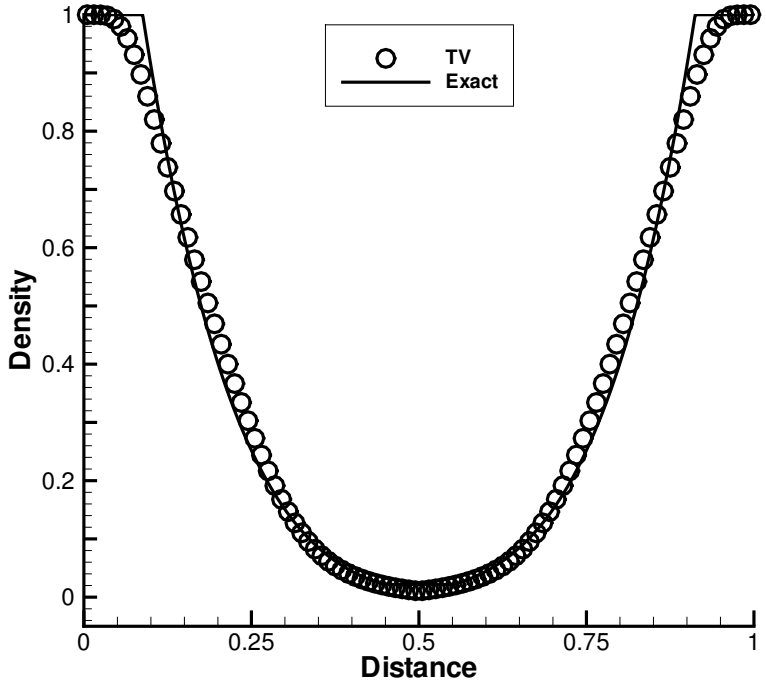

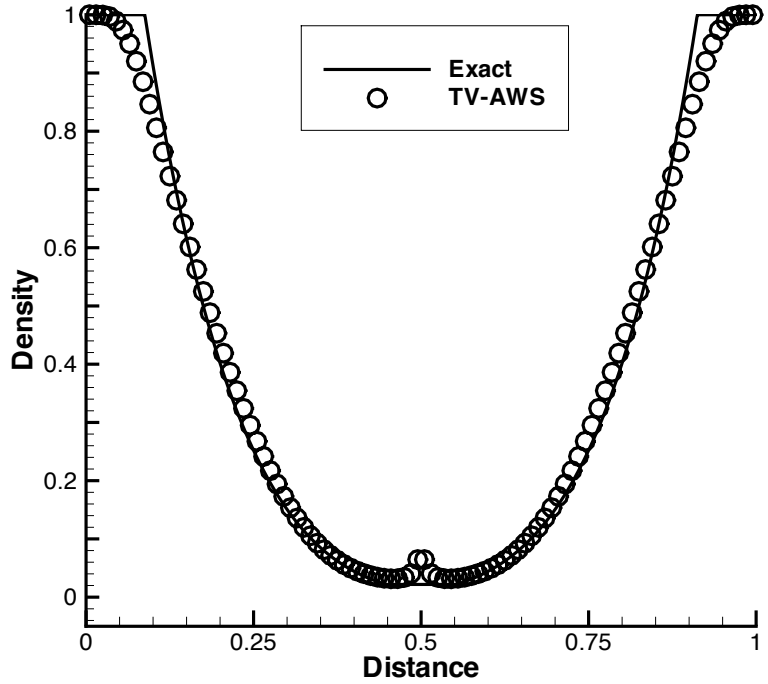

Test 2 (low density). Exact (line) and numerical solutions (symbols) using two numerical schemes (TV and TV-AWS) for the flux splitting of this paper.

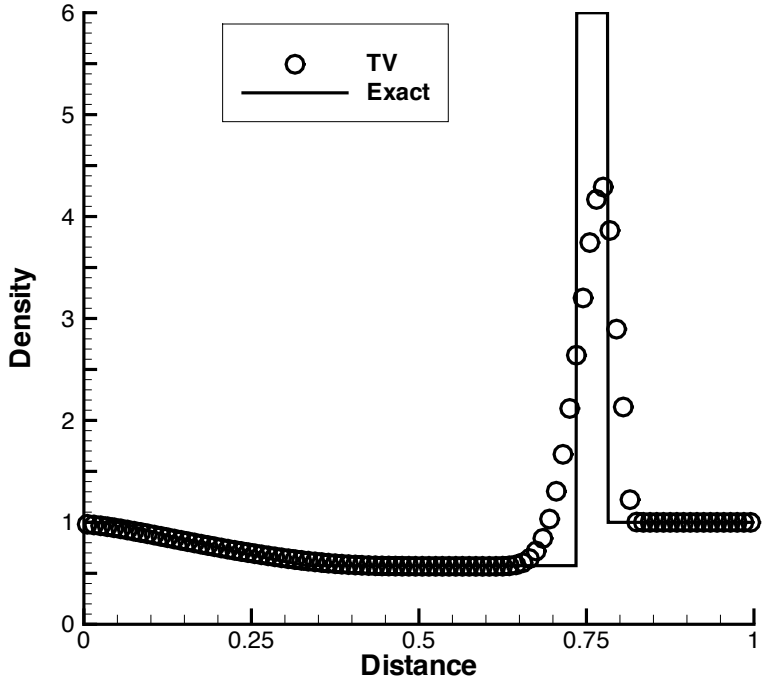

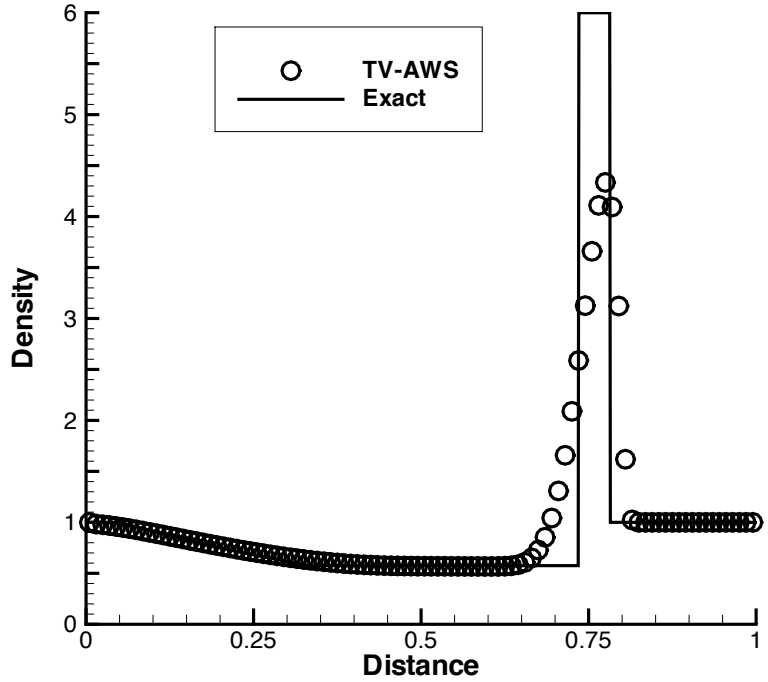

Test 3 (very strong shock). Exact (line) and numerical solutions (symbols) using two numerical schemes (TV and TV-AWS) for the flux splitting of this paper.

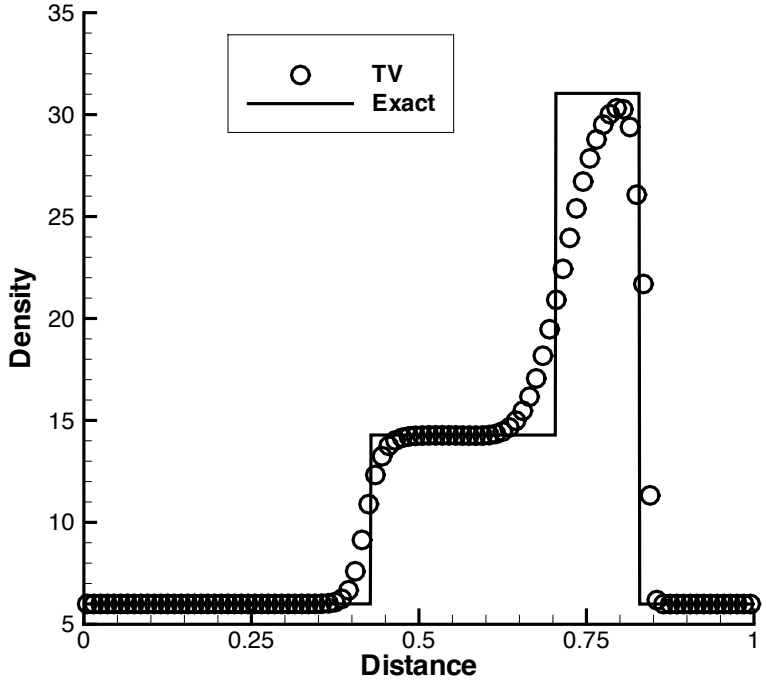

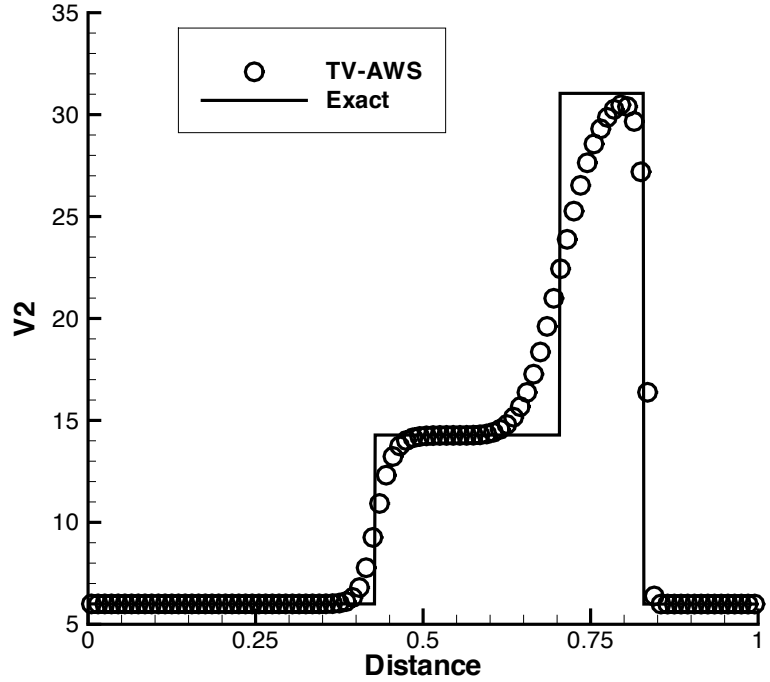

Test 4 (collision of two strong shocks). Exact (line) and numerical solutions (symbols) using two numerical schemes (TV and TV-AWS) for the flux splitting of this paper.

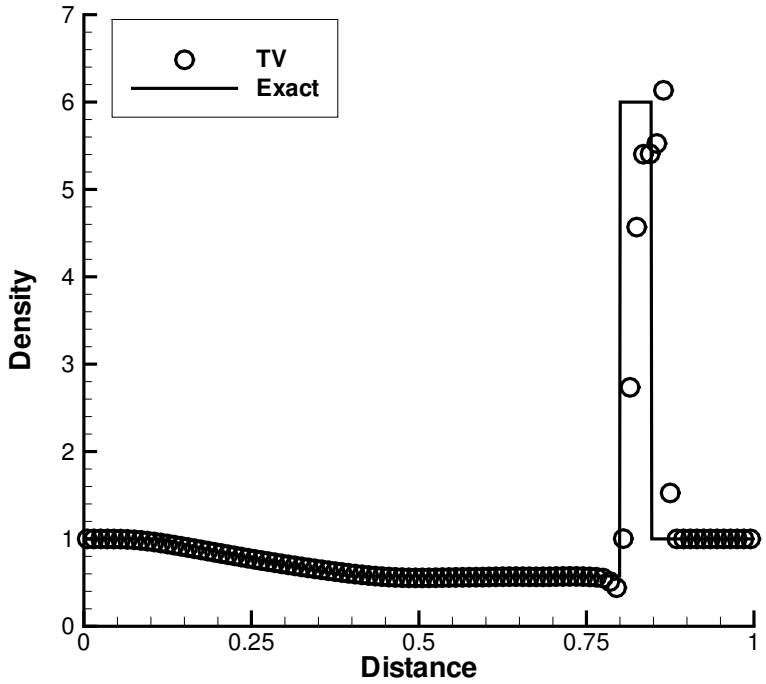

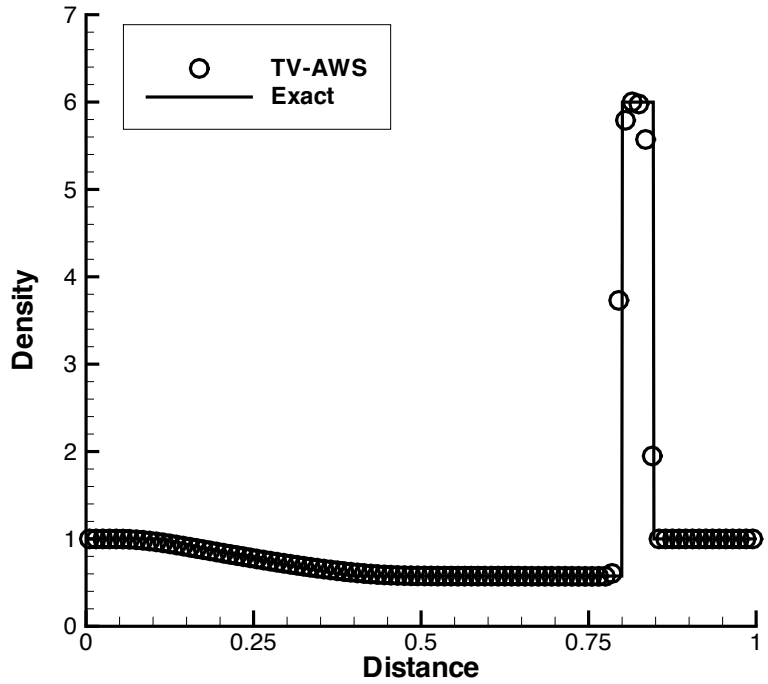

Test 5 (non-isolated stationary contact discontinuity). Exact (line) and numerical solutions (symbols) using two numerical schemes (TV and TV-AWS) for the flux splitting of this paper.

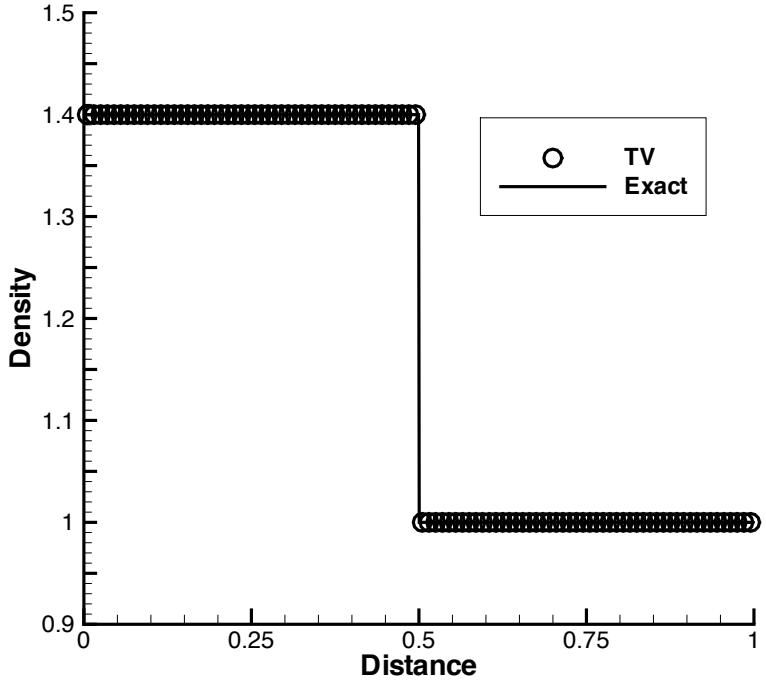

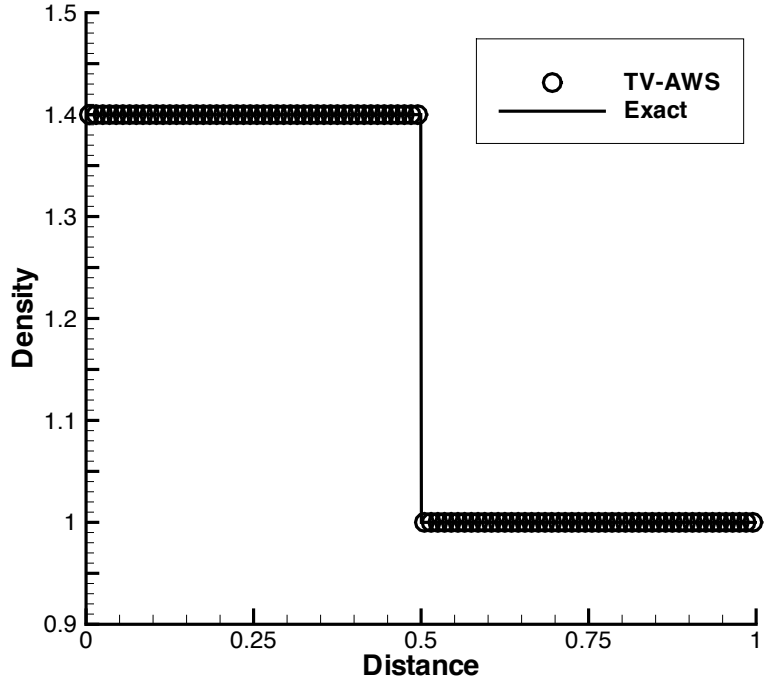

Test 6 (Isolated stationary contact discontinuity). Exact (line) and numerical solutions (symbols) using two numerical schemes (TV and TV-AWS) for the flux splitting of this paper.

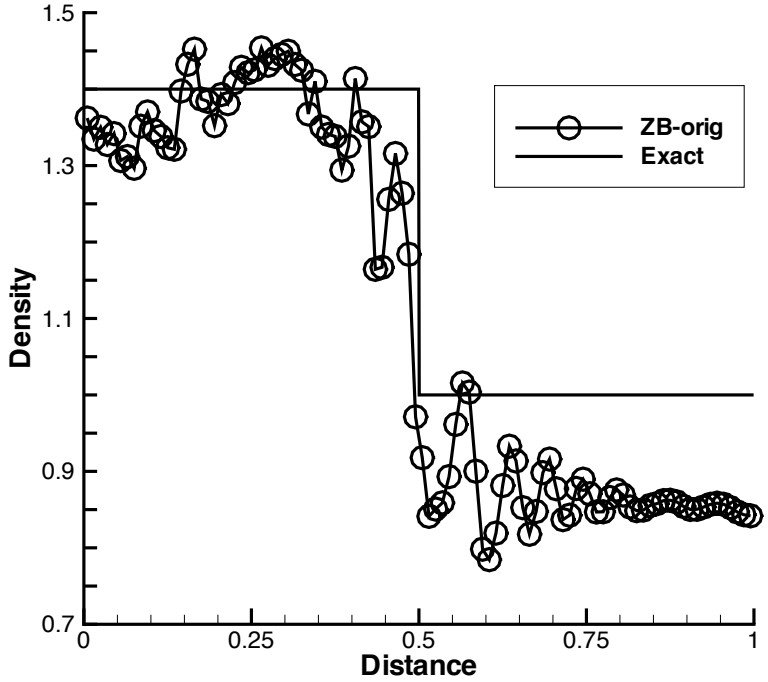

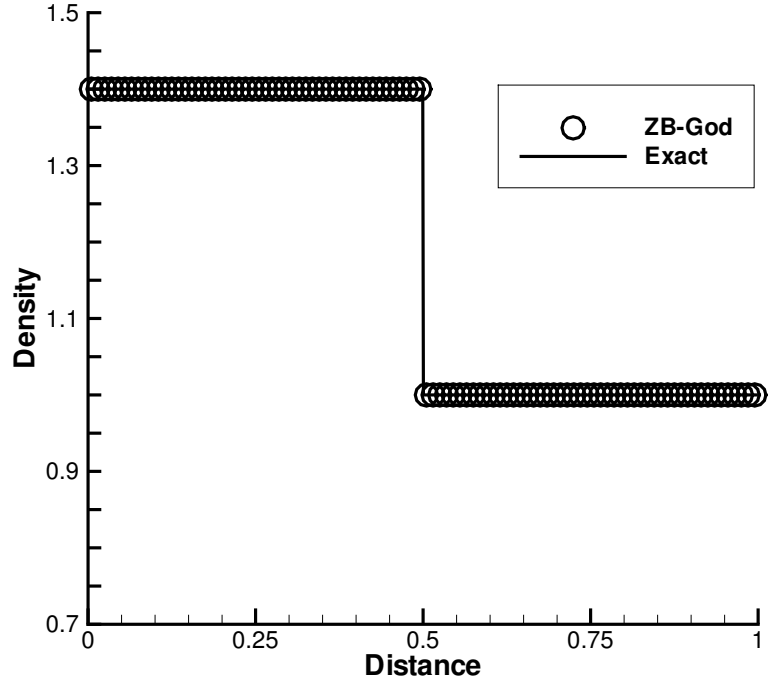

Test 6 (Isolated stationary contact discontinuity). Exact (line) and numerical solutions (symbols) using two numerical schemes: the Zha-Bilgen original scheme (ZB-orig) and the Zha-Bilgen splitting with present Godunov-type numerical approach (ZB-God).

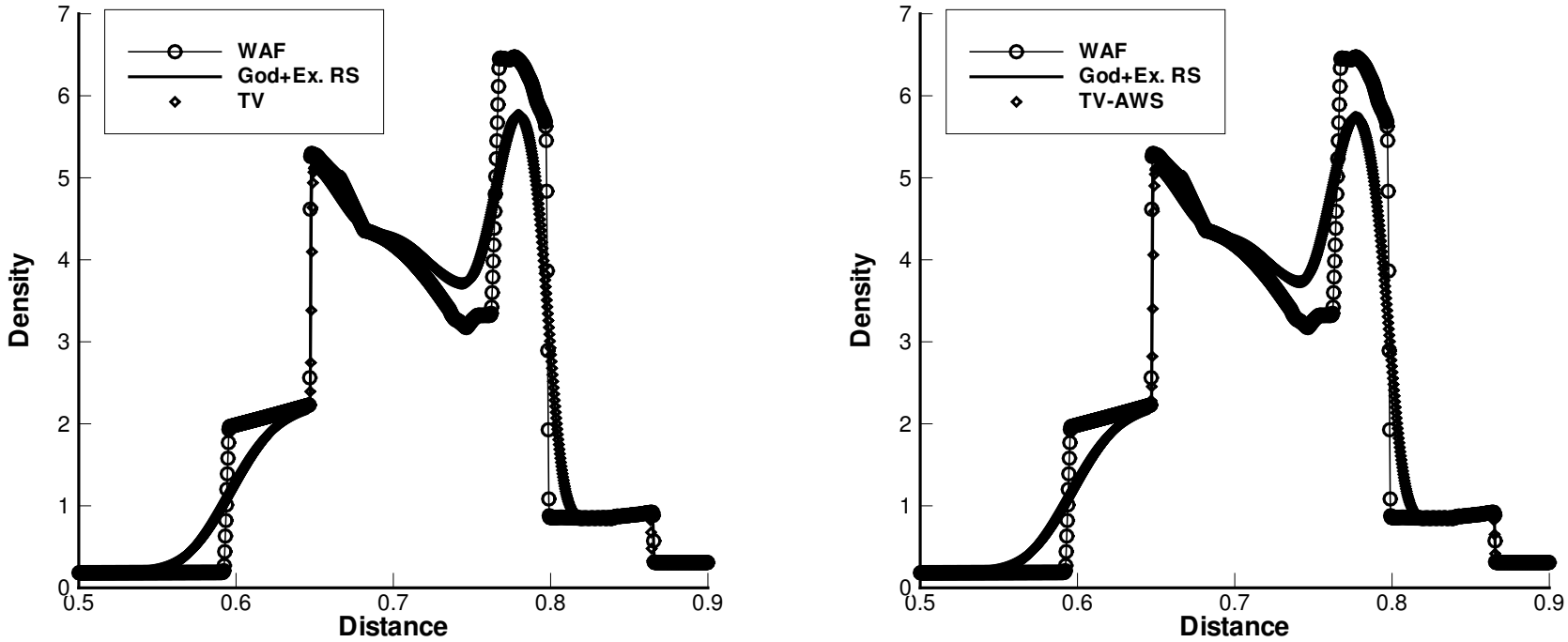

Test 7 (Woodward and Colella blast wave problem). Reference solutions (WAF and Godunov's method with exact Riemann solver) and numerical solutions from two numerical schemes of this paper: TV (top) and TV-AWS (bottom).

Other Potential Schemes for the Pressure System

- Lax-Friedrichs
- FORCE
- Rusanov
- HLL
- Godunov Centred

Part B: Concluding Remarks

- New flux splitting
- New way of dealing with pressure term
- Scheme captures contact discontinuity as well as AUSM
- Our scheme is more robust and more accurate than AUSM
- Other schemes for pressure system under study
- Best combination: explicit for advection implicit for pressure

Thank You